Marine Geology 341 (2013) 68–85

Contents lists available at SciVerse ScienceDirect

Marine Geology

journal homepage: www.elsevier.com/locate/margeo

11,000 yrs of environmental change in the Northwest Passage: A multiproxy core record from central Parry Channel, Canadian High Arctic

Anna J. Pieńkowski [a,*], John H. England [b], Mark F.A. Furze [c], Steve Blasco [d], Peta J. Mudie [d], Brian MacLean [d]

[a] School of Ocean Sciences, College of Natural Sciences, Bangor University, Menai Bridge LL59 5AB, UK
[b] Department of Earth & Atmospheric Sciences, University of Alberta, Edmonton, Alberta T6G 2E3, Canada
[c] Earth & Planetary Sciences Division, Department of Physical Sciences, MacEwan University, Edmonton, Alberta T5J 4S2, Canada
[d] Geological Survey of Canada — Atlantic, Dartmouth, Nova Scotia B2Y 4A2, Canada

ARTICLE INFO

Article history:
Received 19 July 2012
Received in revised form 30 March 2013
Accepted 21 April 2013
Available online 1 May 2013

Communicated by G.J. de Lange

Keywords:
Holocene
environmental change
deglaciation
Canadian Arctic Archipelago
microfossils
palynology

ABSTRACT

Piston core 97022-004PC (74° 48.0′N 97°05.9′W; 267 m water depth) represents a rare paleoenvironmental archive from the understudied west-central Canadian Arctic Archipelago. Lithological, biogeochemical, and microfossil (dinoflagellate cysts, non-pollen palynomorphs, benthic and planktonic foraminifera) characteristics, in combination with a chronostratigraphy based on seventeen radiocarbon dates, show seven prominent paleoenvironmental episodes since the end of the last regional glaciation. The basal diamict (Zone I) records decoupling of previously grounded glacial ice, followed by ice-proximal conditions (Zone IIa) commencing at ~10.8 cal ka BP (age-depth model extrapolation). After an interval of pervasive sea-ice (Zone IIb), ice-distal conditions are established (Zone IIc). Although sparse microfossils are present in glaciomarine sediments (Zone II), noticeable biological activity with heightened abundances and diversities across all groups begins in the postglacial Zone III (10.3–10.0 cal ka BP) when planktonic foraminifera (*Neogloboquadrina pachyderma*) appear. As planktonics are excluded from the study area today (due to shallow inter-channel sills), this likely signals the inflow of relatively warm and saline Atlantic-derived Arctic Intermediate Water below 250 m, presumably facilitated by glacio-isostatically enhanced deglacial water depths. The subsequent Zone IV (10.0–7.0 cal ka BP), characterized by heightened biological productivity in both plankton and benthos and reduced seasonal sea-ice cover, may correspond to a previously proposed Holocene Thermal Maximum. This apparent amelioration ends by the mid Holocene (Zone V; 7.0–5.7 cal ka BP) when Arctic Intermediate Water is excluded from the study area and water depths approach modern values. High-Arctic conditions with seasonal sea-ice cover, a circulation dominated by Arctic Ocean Surface Water, and microfossil assemblages similar to modern are found from ~5.7 cal ka BP onwards (Zones VI–VII). As only minor environmental fluctuations are apparent during the late Holocene, shorter-term climatic episodes (e.g. Little Ice Age) are not recognized in this record.

1. Introduction

The Canadian Arctic Archipelago (CAA; Fig. 1A) occupies a fundamental role in global oceanographic circulation, freshwater budgets, and ecosystems (Melling, 2000; Munk, 2003; ACIA, 2005). Like other Arctic regions, marine and terrestrial CAA environments have shown recent shifts, including: sea-level rise, sea-ice decline, and increasing mean annual temperature (ACIA, 2005; IPCC, 2007). Longer term (pre-instrumental measurement) variability is also suggested by regional marine records (MacLean and Vilks, 1986; MacLean et al., 1989; Mudie et al., 2005; Richerol et al., 2008; Schell et al., 2008a; Scott et al., 2009; Vare et al., 2009; Belt et al., 2010; Gregory et al., 2010; Ledu et al., 2010a, 2010b; Pieńkowski et al., 2011; Melling et al., 2012; Pieńkowski et al., 2012), which provide a long-term context for current environmental changes (Bradley and England, 2008; England et al., 2008; Polyak et al., 2010; White et al., 2010). However, the spatial coverage of records from the marine CAA ("Northwest Passage" = NWP; Fig. 1) remains limited, and important deglacial–postglacial changes (Laurentide–Innuitian ice sheet decoupling, meltwater outflow, sea-level fluctuations) have been primarily terrestrially-derived (e.g. Hodgson and Vincent, 1984; Dyke and Prest, 1987; Bradley, 1990; Dyke et al., 1991; Gajewski, 1995; Dyke et al., 1996a, 1996b; Dyke, 2004; England et al., 2006, 2009).

To improve the spatial and temporal resolution of CAA marine data, we present a chronologically well-constrained, long-term record from west-central Parry Channel, extending to deglaciation (~11 cal ka BP), from a critical decoupling zone between Innuitian and Laurentide ice sheets (Dyke, 2004; England et al., 2006). Core 9722-004PC (Fig. 1) was studied for lithology, macro- and microfossils; previous work on this record includes a qualitative foraminiferal assay and eight ^{14}C dates (Blasco et al., 2005). This study elucidates the regional marine

---

* Corresponding author. Tel.: +44 1248 382858.
E-mail address: a.pienkowski@bangor.ac.uk (A.J. Pieńkowski).

0025-3227/$ – see front matter. Crown Copyright © 2013 Published by Elsevier B.V. All rights reserved.
http://dx.doi.org/10.1016/j.margeo.2013.04.008

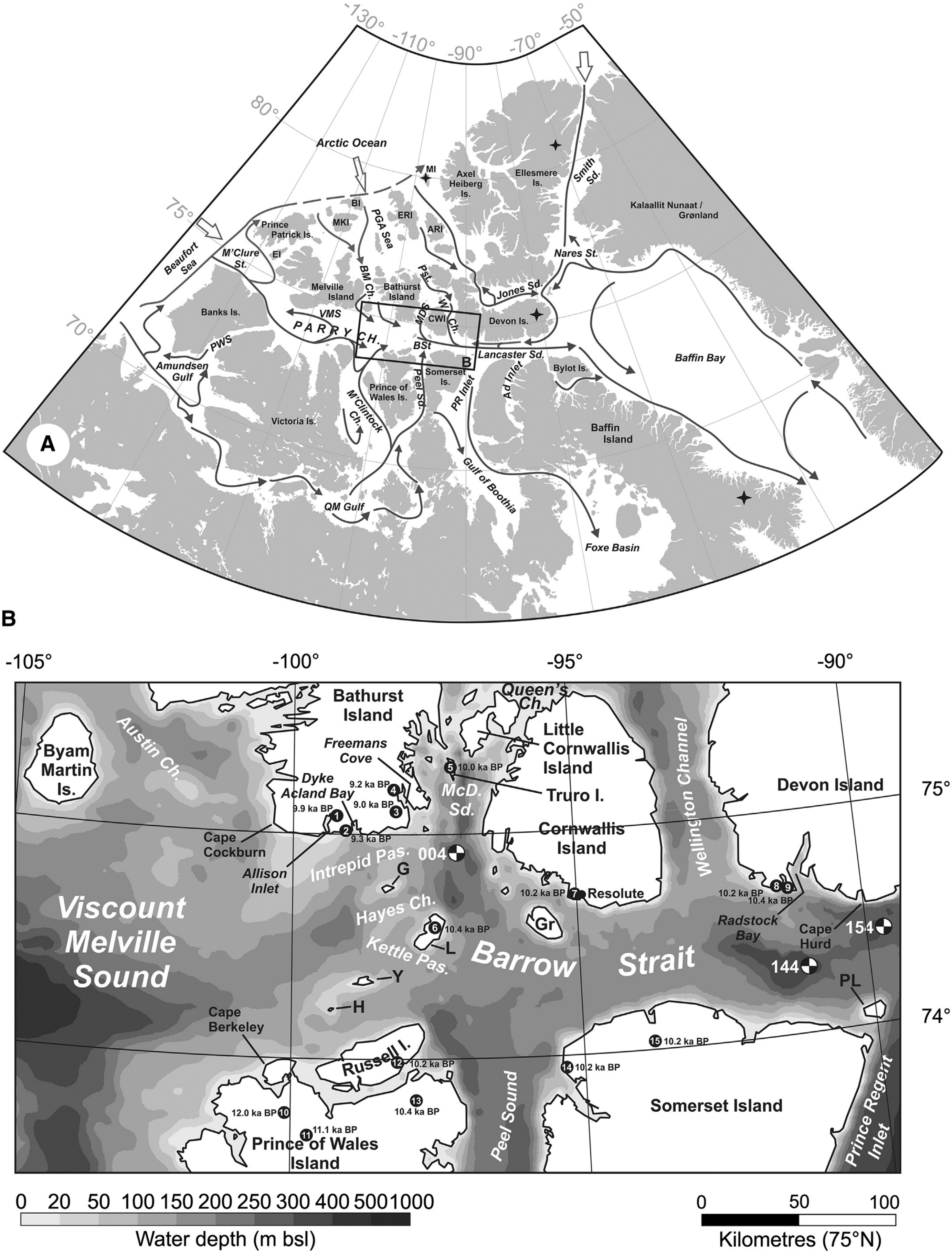
-130°
-110°
-90°
-70°
-50°
80°
75°
70°
Arctic Ocean
MI
Axel Heiberg Is.
Ellesmere Is.
Smith Sd.
Kalaallit Nunaat / Grønland
BI
MKI
PGA Sea
ERI
ARI
Prince Patrick Is.
EI
Beaufort Sea
M'Clure St.
Nares St.
Melville Island
BM Ch.
Bathurst Island
PSt.
W. Ch.
Jones Sd.
MDS
CWI
Devon Is.
Banks Is.
VMS
PARRY CH.
BSt
Lancaster Sd.
B
PWS
Amundsen Gulf
Somerset Is.
Prince of Wales Is.
Peel Sd.
PR Inlet
Ad Inlet
Bylot Is.
Baffin Bay
M'Clintock Ch.
Victoria Is.
Baffin Island
A
Gulf of Boothia
QM Gulf
Foxe Basin
B
-105°
-100°
-95°
-90°
Bathurst Island
Queen's Ch.
Little Cornwallis Island
Byam Martin Is.
Austin Ch.
Freemans Cove
Dyke Acland Bay
9.2 ka BP
4
5 10.0 ka BP
McD. Sd.
Truro I.
Devon Island
75°
9.0 ka BP
3
9.9 ka BP
1
2
9.3 ka BP
Cornwallis Island
Wellington Channel
Cape Cockburn
004
Allison Inlet
Intrepid Pas.
G
10.2 ka BP
7 Resolute
10.2 ka BP
8
9
10.4 ka BP
Viscount Melville Sound
Hayes Ch.
6 10.4 ka BP
Gr
Radstock Bay
Cape Hurd
154
L
Kettle Pas.
Barrow Strait
144
Y
PL
H
74°
Cape Berkeley
15 10.2 ka BP
Russell I.
12 10.2 ka BP
14 10.2 ka BP
13
10.4 ka BP
12.0 ka BP 10
Peel Sound
Somerset Island
11 11.1 ka BP
Prince of Wales Island
Prince Regent Inlet
0 20 50 100 150 200 250 300 400 500 1000
Water depth (m bsl)
0 50 100
Kilometres (75°N)

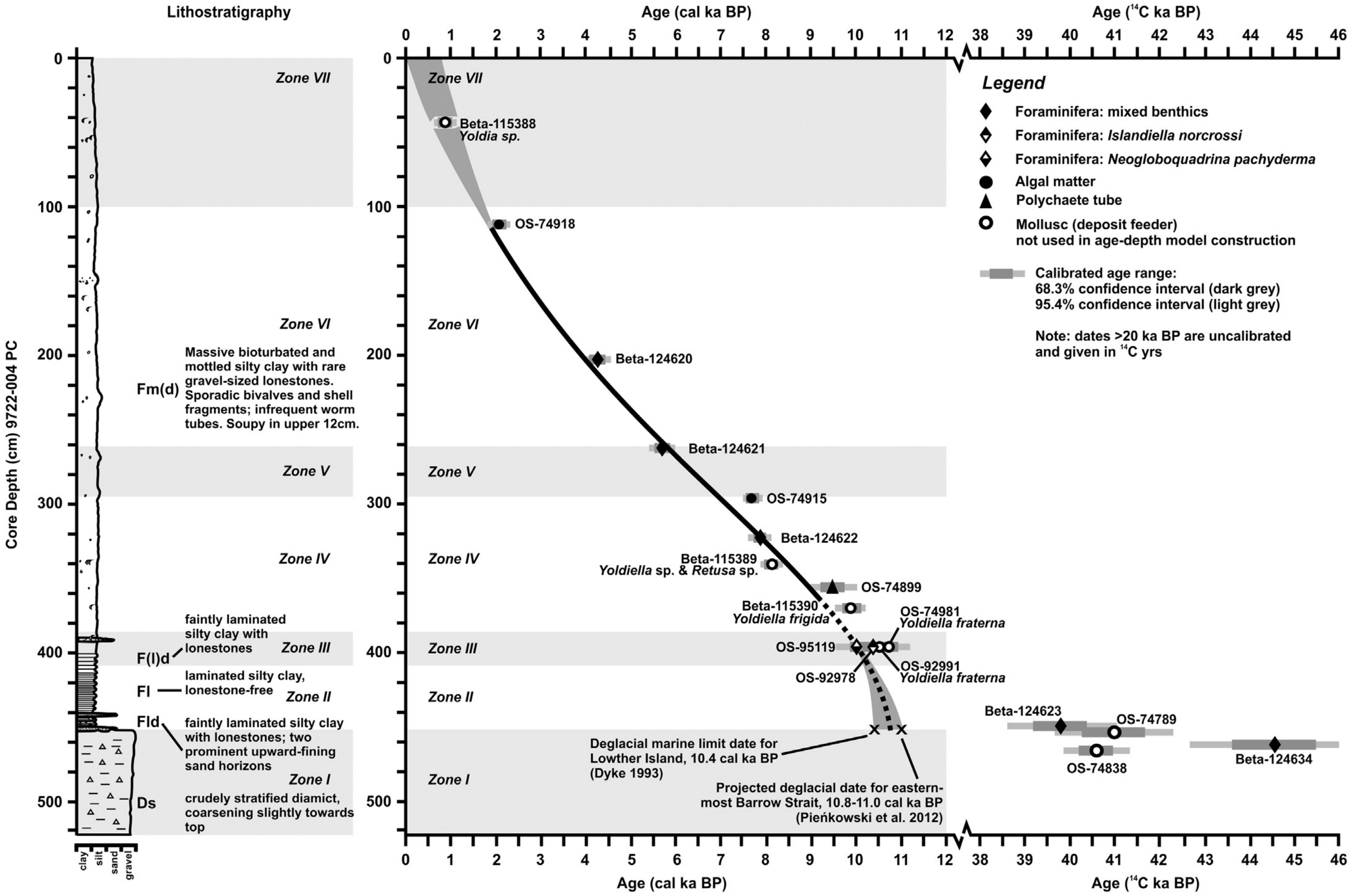

Fig. 2. Core 9722-004PC lithostratigraphy and age-depth model. Lithostratigraphic codes are based on Eyles et al. (1983). Ds = stratified diamict; F = fines; m = massive; l = laminated; (l) = faintly laminated; d = dropstones. Paleoenvironmental Zones (I–VII; distinguished by alternating gray and white bands) were determined according to a combination of litho- and bio-stratigraphic characteristics. The age-depth model is based on eight calibrated radiocarbon dates. Dates on detrital-feeding molluscs not used in age-depth model construction are shown for comparison only. Dates >20 ka BP are uncalibrated. Details of radiocarbon dates can be found in Table 1.

terval, complementing and expanding the terrestrial record and advancing our understanding of the late Quaternary evolution of Arctic North America.

2. Regional setting

Parry Channel, the main geographic NWP axis (Pharand, 1984), comprises several interlinked waterways. Barrow Strait is flanked to the west by Viscount Melville Sound and M'Clure Strait, and to the east by Lancaster Sound (Fig. 1A). Net circulation is southeastward from the western Arctic Ocean (Canada Basin) to Baffin Bay, though both Pacific- and Atlantic-origin waters occur within the CAA (Ingram and Prinsenberg, 1998; Michel et al., 2006). Modern circulation is controlled by numerous shallow sills limiting deep water inflow. The Lowther–Young islands sill (~125 m; Fig. 1B) permits Arctic Ocean Surface Water (AOSW; Melling, 2000; Melling et al., 2012) throughflow from Canada Basin but restricts entry of Arctic Intermediate Water and M'Clure Strait (Jones and Coote, 1980; Coote and Jones, 1982; Tang et al., 2004). Pacific-derived AOSW occurs throughout Barrow Strait (Jones et al., 2003; Michel et al., 2006) whereas Atlantic water flows westward into Parry Channel (Baffin Bay Atlantic Water = BBAW; Leblond, 1980; Rudels, 1986), mixing with eastward-flowing Barrow Strait AOSW (BBAW/AOSW; Tang et al., 2004; Michel et al., 2006).

Piston core 9722-004PC was recovered in northwestern Barrow Strait adjacent to McDougall Sound (Fig. 1B). The site receives AOSW via Viscount Melville Sound (west) and Penny Strait (north), whose waters are more saline and colder (>32.8 salinity, −1.77 °C at 10 m depth; Prinsenberg and Bennett, 1987). Warmer, fresher water which flows in via Peel Sound (south; Fig. 1A) diverges eastward, around northern Somerset Island (Prinsenberg and Bennett, 1987). Strong tidal currents (50–150 cm/s) around shallow sills contribute to waters mixing *en route* to Baffin Bay (Melling, 2000). First-year fast ice dominates this region, with freeze-up in late September/early October and break-up by mid-July (Pharand, 1984; Barry, 1993; Michel et al., 2006). Open

Fig. 1. (A) Map of the Canadian Arctic Archipelago (CAA) showing the generalized oceanographic circulation (after Ingram and Prinsenberg, 1998). Ice core locations referred to in the text are denoted by a star (✦), including the Agassiz Ice Cap (Ellesmere Island), the Penny Ice Cap (Baffin Island), the Devon Ice Cap (Devon Island), and the Meighen Ice Cap (Meighen Island). Abbreviations: AD Inlet = Admiralty Inlet; ARI = Amund Ringnes Islands; BI = Borden Island; BM Ch. = Byam Martin Channel; BSt = Barrow Strait; CWI = Cornwallis Island; EI = Eglington Island; ERI = Ellef Ringnes Island; MDS = McDougall Sound; MI = Meighen Island; MKI = Mackenzie King Island; PGA Sea = Prince Gustav Adolf Sea; PR Inlet = Prince Regent Inlet; PSt = Penny Strait; PWS = Prince of Wales Strait; QM Gulf = Queen Maud Gulf; VMS = Viscount Melville Sound; W Ch. = Wellington Channel. (B) Detailed inset of the core site 9722-004 ("004"), including bathymetry (based on Jakobsson et al., 2008), deglacial dates in cal ka BP (numbers in black circles correspond to dates in Table 2), and deglacial to Holocene long cores 86027-144 ("144"; Pieńkowski et al., 2012) and 86027-154 ("154"; Pieńkowski et al., submitted for publication). Abbreviations: McD. Sd. = McDougall Sound.

water allows multi-year pack-ice to enter western Barrow Strait via McDougall Sound (Melling, 2002), as observed recently (Michel et al., 2006; Howell et al., 2009).

3. Materials and methods

3.1. Core materials & sediment properties

Piston core 9722-004PC ("004PC"), retrieved at 74° 48.0′N 97°05.9′ W (267 m water depth; Fig. 1B) by the Geological Survey of Canada (GSC)-Atlantic (Hurlbut, 1997), consists of ~400 cm of massive silty clay overlying laminated clays (404–453 cm) and diamicton (453–523 cm; Fig. 2). Similar sediment sequences have been interpreted as i) massive, fine-grained postglacial sediments overlying; ii) ice-proximal to -distal laminated glaciomarine sediments deposited by a retreating grounded glacier and/or beneath ice shelves; and iii) "glacial drift" — till derived from grounded ice or ice-proximal deposition (MacLean et al., 1989; Andrews et al., 1991; Pieńkowski et al., 2012).

Magnetic susceptibility (MS), density and grain size (Beckman Coulter LS230 laser diffraction instrument; range 0.4–2000 μm) were measured at GSC-Atlantic. Percentages of lithoclasts > 125 μm to 2 mm and > 2 mm relative to total dry weight were used to determine coarse sediment input and ice rafting (either glacial or sea-ice). For biogenic silica (BioSil) content (%), oven-dried (45 °C) and powdered sediment samples (~2 g) were measured by the Pacific Centre for Isotopic and Geochemical Research (University of British Columbia) following Mortlock and Froelich (1989). Sedimentation rates were derived from the age-depth model (Section 3.3).

3.2. Chronostratigraphy

Seventeen AMS (Accelerator Mass Spectrometry) ^{14}C dates were obtained (Table 1; eight pre-existing, nine new dates) and all were calibrated in CALIB 6.0 (Stuiver et al., 2013), using Marine09 (Reimer et al., 2009), and a CAA ΔR of 335 ± 85 yrs (Coulthard et al., 2010). Dates older than the Last Glacial Maximum (LGM; > 18 ^{14}C ka BP) fall beyond, and hence preclude the use of, the Marine09 curve.

Seven radiocarbon dates were based wholly or partially on identified deposit-feeding molluscs (*Yoldiella* spp., *Yoldia* sp.; Ockelmann, 1958), which suffer non-systematically from enhanced apparent age effects ('Portlandia Effect') due to uptake of 'old' detrital carbon from carbonate bedrock (cf. Forman and Polyak, 1997; England et al., 2012). As expected, most of these dates plot older than the age-depth curve, and were excluded from age-depth model construction; nonetheless, they are plotted (Fig. 2) for comparison with non-Portlandia Effect samples. At 395–397 cm depth, dates on detrital-feeding molluscs and benthic and planktonic foraminifera allow direct comparison between different materials (Table 1). The two *Yoldiella fraterna* dates are consistently older than foraminiferal dates (as expected) though a ~380 cal yrs difference exists between benthic and planktonic foraminiferal dates, the benthic *Islandiella norcrossi* appearing older. Such differences may arise from time averaging, species-specific effects, or watermass ventilation histories (depth-variable ΔR).

For further comparisons of the 004PC chronology with regional (raised marine) ages, previously published dates were calibrated using the same protocol (above). Where appropriate, such land-based dates were first "de-corrected" for prior reservoir correction (GSC dates post 1992; Coulthard et al., 2010). Dates originally normalized to δ^{13}C of 0‰ were converted to the equivalent conventional radiocarbon age (normalized to −25‰ δ^{13}C; sensu Stuiver and Polach, 1977) by adding 400 ^{14}C yrs (Coulthard et al., 2010). Marine mammal dates were calibrated using the above methodology, with a ΔR of 170 ± 95 yrs for bowhead whale (*Balaena mysticetus*; Furze et al., submitted for publication) and a ΔR of 335 ± 85 yrs for walrus (*Odobenus rosmarus*) given their molluscan diet (cf. Coulthard et al., 2010). Molluscan ages > 10.5 ^{14}C ka BP were provisionally calibrated using ΔR of 1000 yrs due to presumably limited Arctic Ocean ventilation during, and prior to, the Younger Dryas (Hanslik et al., 2010).

3.3. Age-depth model

A best-fit (fourth-order polynomial) curve was plotted through CALIB 6.0 median probability ages and associated 95.4% probability age ranges against core depth (Fig. 2). The curve excluded all samples with the Portlandia Effect; a previously dated mixed sample on deposit-feeding bivalves and a predatory opisthobranch gastropod (Beta-115389); and four considerably older (> 37,000 ^{14}C yrs) basal dates incorporating reworked pre-Late Wisconsinan material (Fig. 2; Table 1).

Beyond the ages obtained on the uppermost and lowermost (post-glacial) non-deposit feeder samples, the polynomial curve is extrapolated. Towards the core base, linear extrapolation to the

Table 1

Radiocarbon dates from core 9722-004PC. All radiocarbon dates have been normalized to a δ^{13}C value of −25‰ (Stuiver and Polach, 1977). Dates were calibrated in CALIB 6.0 (Stuiver et al., 2013) based on the marine calibration dataset Marine09 (Reimer et al., 2009), with a ΔR of 335 ± 85 yrs applicable to the CAA (Coulthard et al., 2010). Ages > 18 ^{14}C ka BP (in italics) were left uncalibrated, being beyond the range of the Marine09 calibration data set.

Core depth (cm)	Laboratory code	Material dated	Machine age ± 1σ (^{14}C yrs BP)	δ^{13}C (‰)	68.2% range (cal yrs BP) probability 1	95.4% range (cal yrs BP) probability 1	Calib median probability age (cal yrs BP) rounded to nearest 10 cal yrs
43–45	Beta-115388	Bivalve *Yoldia* sp.	1660 ± 50	0.70	754–959	668–1068	870
109–114	OS-74916	Macro-algal matter	2790 ± 30	−17.42	1987–2240	1889–2315	2110
201–203	Beta-124620	Mixed benthic foraminifera	4550 ± 50	−1.70	4153–4426	4004–4570	4300
261–263	Beta-124621	Mixed benthic foraminifera	5690 ± 80	−0.60	5607–5852	5472–5973	5730
295–297	OS-74915	Macro-algal matter	7590 ± 45	−18.36	7625–7819	7557–7919	7730
321–323	Beta-124622	Mixed benthic foraminifera	7770 ± 40	−1.70	7795–7987	7688–8099	7890
340	Beta-115389	Bivalve *Portlandia frigida* & Gastropod *Retusa* sp.	8000 ± 50	0.00	8007–8226	7938–8331	8130
355–357	OS-74899	Polychaete tube	9150 ± 160	−22.98	9255–9728	9023–10,011	9500
370	Beta-115390	Bivalve *Portlandia frigida*	9460 ± 40	0.80	9739–10,071	9593–10,155	9890
395–397	OS-92978	Benthic foraminifera *Islandiella norcrossi*	9880 ± 35	−1.01	10,294–10,501	10,211–10,567	10,400
395–397	OS-95119	Planktonic foraminifera *Neogloboquadrina pachyderma*	9560 ± 70	−0.05	9878–10,184	9651–10,273	10,010
395–397	OS-92991	Bivalve *Yoldiella fraterna*	9980 ± 50	0.41	*10,382–10,600*	*10,238–10,723*	*10,500*
395–397	OS-74981	Bivalve *Yoldiella fraterna*	10,150 ± 95	0.19	*10,548–10,911*	*10,463–11,113*	*10,740*
448–450	Beta-124623	Mixed benthic foraminifera	39,790 ± 550	0.50	*42,808–43,758*	*42,438–44,225*	*43,290*
455–457	OS-74789	Bivalve *Yoldiella fraterna*	41,000 ± 630	0.56	*43,628–44,669*	*43,108–45,129*	*44,160*
459–463	Beta-124634	Mixed benthic foraminifera	44,540 ± 860	1.50	*45,886–47,880*	*45,394–49,130*	*46,990*
465–467	OS-74838	Bivalve *Yoldiella fraterna*	40,600 ± 330	0.35	*43,551–44,224*	*43,206–44,489*	*43,880*

Table 2
Mollusc-based deglacial dates from the coasts of central Parry Channel (locations shown in Fig. 1B). ^{14}C dates were calibrated using CALIB 6.0 (Stuiver et al., 2013) based on the marine calibration data set Marine09 (Reimer et al., 2009), with a ΔR value of 335 ± 85 yrs (<10,500 ^{14}C yrs BP; Coulthard et al., 2010) or 1000 yrs (>10,500 ^{14}C yrs BP; Hanslik et al., 2010). Dates indicated by * were first 'de-corrected' for any prior reservoir correction (GSC dates post-1992; Coulthard et al., 2010) or, where originally normalized to a δ^{13}C ratio of 0‰, converted to the equivalent of a conventional radiocarbon age (normalized to −25‰ δ^{13}C; sensu Stuiver and Polach, 1977) by adding 400 ^{14}C yrs (Coulthard et al., 2010).

Site no.	Location	Laboratory code	Material dated	Published age ± 1σ (^{14}C yrs BP)	Elevation (m)	Marine limit (m)	68.2% range (cal yrs BP) probability 1	95.4% range (cal yrs BP) probability 1	Calib 6.0 median probability age (cal yrs BP) to nearest 10 yrs	Latitude	Longitude	Reference
1	Bathurst I., Allison Inlet	GSC-353	*Hiatella arctica*	9070 ± 190	104	≥104	9632–10,155	9427–10,405	9890	75° 06′ N	99° 08′ W	Dyke et al. (1991)
2	Bathurst I., Dyke Acland Bay	GSC-250	*Hiatella arctica*	8590 ± 140	107	110	9110–9480	8865–9691	9290	75° 0.3′ N	98° 59.7′ W	Bednarski (2003)
3	Bathurst I., Freemans Cove	GSC-6353	*Mya truncata* & *Hiatella arctica*	8750 ± 110	98	107	8803–9232	8616–9376	9010	75° 7.8′ N	98° 6.2′ W	Bednarski (2003)
4	Bathurst I., Round Hill	GSC-191	*Mya truncata*	8520 ± 150	98	–	9022–9420	8715–9581	9210	75° 12.1′ N	98° 5.9′ W	Bednarski (2003)
5	Truro I., east side	GSC-722	*Mya truncata* & *Hiatella arctica*	9160 ± 160	~107	>107	9741–10,224	9531–10,426	9990	75° 19′ N	97° 10′ W	Washburn and Stuiver (1985)
6	Lowther I.	GSC-322	*Hiatella arctica*	9470 ± 150	113–119	–	10,202–10,561	9910–10,880	10,390	74° 33′ N	97° 31′ W	Washburn and Stuiver (1985)
7	Cornwallis I., Resolute Bay	QL-1751	*Hiatella arctica* & *Balanus balanus*	9690 ± 90	113	120	10,037–10,380	9834–10,503	10,190	74° 42.7′ N	94° 52′ W	Washburn and Stuiver (1985)
8	Devon I., Radstock Bay	GSC-1502	*Balanus balanus*	9260 ± 150*	105	>107	9903–10,374	9652–10,531	10,130	74° 40′ N	91° 25′ W	Dyke et al. (1991)
9	Devon I. Gascoyne Inlet	GSC-5940	*Hiatella arctica*	9470 ± 90*	115	115	10,255–10,506	10,138–10,639	10,390	74° 39.3′ N	91° 17.9′ W	Dyke (1999)
10	Prince of Wales I. northwestern	S-2708	*Hiatella arctica*	11,005 ± 170	133	≤188	11,652–12,367	11,329–12,558	11,970	73° 47′ N	99° 46′ W	Dyke (1987)
11	Prince of Wales I. Arabella Bay	S-2709	*Hiatella arctica*	10,435 ± 160	120	~120	10,749–11,252	10,573–11,651	11,060	73° 39′ N	99° 30′ W	Dyke (1987)
12	Russell I., eastern end	GSC-3994	Shell	9360 ± 150*	84.5	95	10,104–10,509	9739–10,622	10,270	73° 55′ N	98° 14′ W	Dyke et al. (1991)
13	Prince of Wales I. Cape Hardy	S-2710	Shell	9845 ± 150	95	95	10,186–10,545	9869–10,799	10,360	73° 47.5′ N	97° 42′ W	Dyke et al. (1991)
14	Somerset I., Cape Anne	GSC-319	Shell	9380 ± 180*	121	122	10,076–10,551	9671–10,746	10,280	73° 53.5′ N	95° 19′ W	Dyke et al. (1991)
15	Somerset I., Cunningham Inlet	GSC-150	Shell	9180 ± 170*	62	122	9739–10,248	9539–10,466	10,020	73° 59′ N	93° 40′ W	Dyke et al. (1991)

boundary between laminated (glaciomarine) and diamictic (~glacial) facies provides an age of ~11.8 cal ka BP for deglaciation, older than the well-constrained chronologies from adjacent island coastlines (Dyke, 1993; Bednarski, 2003). The lithology of the basal core units (ice-proximal rhythmites, diamictons) suggests elevated sedimentation rates (Cowan et al., 1997) and thus steepening of the age-depth curve, consistent with fourth-order polynomial extrapolation. Towards the core top, the only date available (44 cm; Beta-115388; 870 cal yrs BP) is on a deposit-feeding mollusc. Given the propensity of deposit-feeding molluscs for enhanced age effects (England et al., 2010), this date should be regarded with caution, but can be used as a maximum age. Projection of the age-depth model (Fig. 2) defines a core-top age range between 0 yrs BP (youngest possible age) and 750 yrs BP (constrained by Beta-115388). An age closer to 750 yrs BP is more consistent with loss of upper seabed sediments during piston coring. The absence of calcareous foraminifera or molluscs, and thus lack of chronological control, prevents a meaningful investigation of the accompanying trigger weight core (97022-004TWC; Hurlbut, 1997). However, previous qualitative (>63 μm) foraminiferal analyses on this record (Blasco et al., 2005) confirm that the top ~100 cm of 004PC is similar to 004TWC, both being dominated by agglutinated faunas.

Marine limit (highest deglacial sea-level) ages from nearby coastlines and marine deglacial dates further constrain the age-depth model. The east–west progression of deglaciation through eastern and central Parry Channel (Dyke et al., 1991; Dyke, 2004) suggests ice lift-off and fragmentation at the study site at, or after, ~11.0 cal ka BP, as established for eastern Parry Channel (Pieńkowski et al., 2012). Given its location, deglaciation of the study site must predate the 10.4 cal ka BP marine limit on Lowther Island (Table 2), where striations suggest a short-lived local ice cap after Laurentide retreat (thus ice break-up and glaciomarine conditions), but before emplacement of the 10.4 cal ka BP shoreline (≈9.5 ^{14}C ka BP; Dyke, 1993). Assuming steepening of the age-depth curve on sedimentological grounds, and using

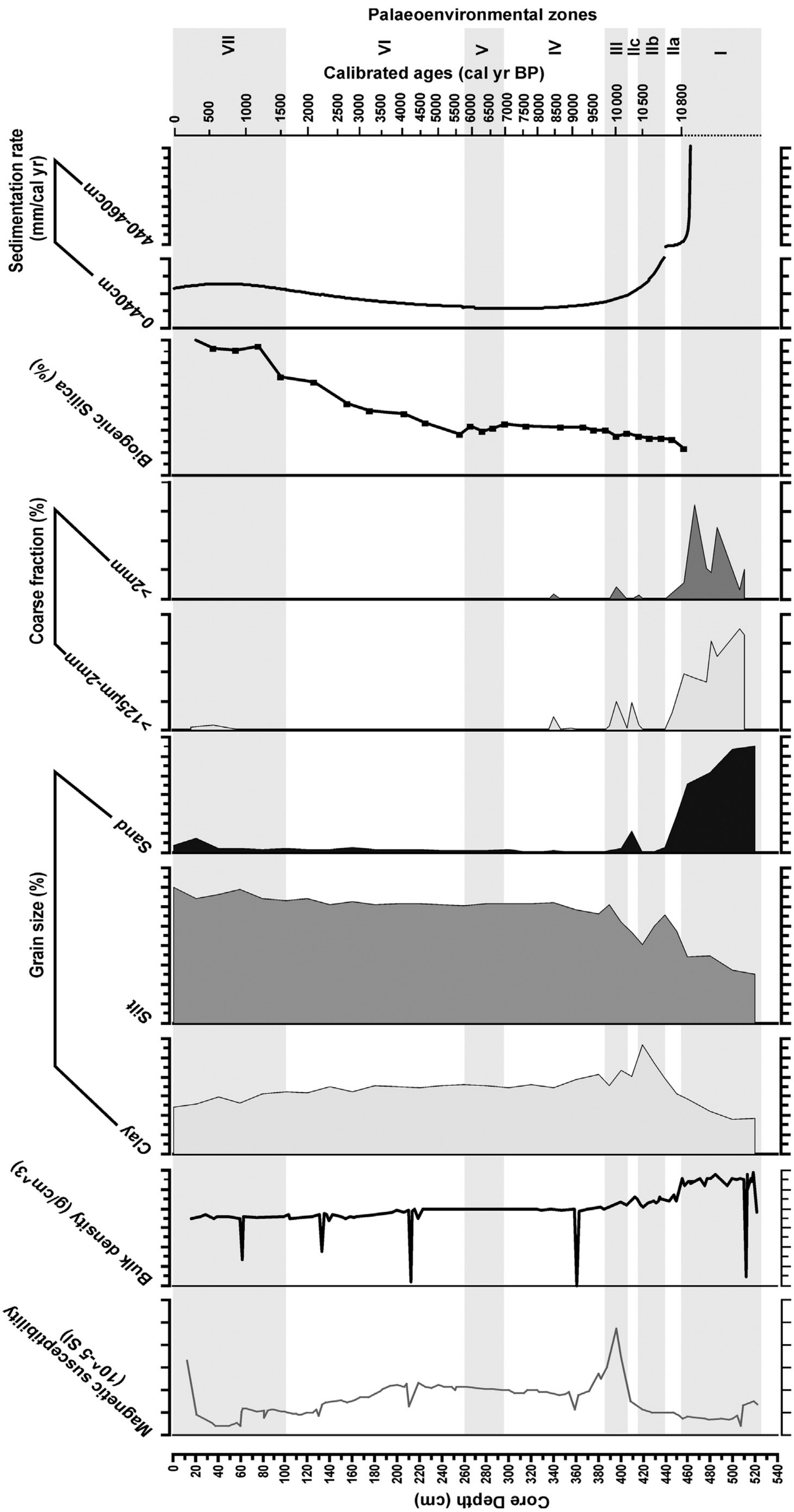

Fig. 3. Results of sedimentological analyses on core 9722-004PC, including magnetic susceptibility, bulk density, % grain size, % coarse fraction contribution (determined from foraminiferal subsamples), and biogenic silica. The age-depth relationship is given according to the age-depth model (Fig. 2).

regional deglacial dates for maximum and minimum ages, the fourth-order polynomial suggests deglaciation (transition laminated to diamictic sediments, 453 cm; Sections 5.1–5.2) at ~10.8 cal ka BP, fully compatible with the comprehensive terrestrial deglacial chronology.

3.4. Microfossils

Samples (~5 cm^3; 5–20 cm intervals) for organic microfossil analyses (dinoflagellate cysts = dinocysts, other non-pollen palynomorphs = NPPs) were wet-weighed, oven-dried (40 °C), and wet-sieved at 125 μm with distilled water. The <125 μm fraction was processed by repeated digestion in 38% cold hydrofluoric and 10% cold hydrochloric acids, followed by sieving at 10 μm with distilled water (Marret and Zonneveld, 2003; protocol 1). *Lycopodium clavatum* tablets (batch #483,216; $x = 18{,}583 \pm 3820$) were added to samples prior to 125 μm wet-sieving to permit calculation of palynomorph concentrations (Stockmarr, 1971), given in number of palynomorphs per dry gram of sediment. Organic residues were mounted in safranin-stained glycerine jelly and systematically scanned under light-transmitted microscopy (×400). Wherever possible, ≥300 dinocysts were counted per sample (average count: 150 cysts), noting any co-occurring NPPs. Palynomorphs were identified using de Vernal et al. (1989), Kunz-Pirrung (1998), Rochon et al. (1999), Head et al. (2001), Roncaglia (2004), and Pieńkowski et al. (2011, 2012). Folded, smooth-walled, round brown cysts not certainly identified as *Brigantedinium* spp. were grouped as *Protoperidinium* spp. Spiny, brown cysts not confidently identified as *Islandinium minutum* were grouped as cf. *I. minutum*. Within *Polykrikos*, Arctic morphotypes (M1, M2), *Polykrikos* sp. A (cf. Mudie and Short, 1985), and *Polykrikos* sp. S (possessing short, faint crests) were distinguished. *Islandinium cezare* s.l. includes *Islandinium? cezare* and *Echinidinium karaense*. Other NPPs comprise acritarchs (*Halodinium minor*, *Palaeostomocystis subtilitheca*, *Palaeostomocystis fritilla*), freshwater algae, zooplankton remains, and miscellaneous algal filaments/tissues ("phytodebris"). Acritarchs of unknown biological affinity include Acritarch P (similar to Cyst P of Scott et al., 1984; after Pieńkowski et al., 2011, 2012), and Acritarch Q (Pieńkowski et al., 2011). Microforaminiferal linings, classified sensu Stancliffe (1991), included biserial (forms A, B), trochospiral (chambers discrete: C; chambers overlap: D), planispiral forms (chambers discrete: E), and miscellaneous others (F).

The >125 μm fraction of sieved samples was oven-dried (40 °C), and examined for calcareous micro- (benthic, planktonic foraminifera; ostracods), and macro-fossils (molluscs, macro-algal matter, worm tubes) with binocular microscopy. foraminifera were identified following Vilks (1969, 1989). *I. norcrossi*, *Islandiella helenae*, and *Cassidulina neoteretis* (sensu Seidenkrantz, 1995) are separated (contrary to Scott et al., 2009; Gregory et al., 2010). *Islandiella* spp. includes all foraminifera not confidently identified to species level (likely *I. norcrossi* or *I. helenae*) due to breakage/dissolution. *Neogloboquadrina pachyderma* [=*N. pachyderma* sinistral (Ehrenberg, 1861)] is defined sensu Darling et al. (2006). Though likely unrepresentative of the total foraminiferal fauna, >125 μm microfossils complement palynomorph and sedimentary analyses.

4. Results

4.1. Sediment properties

Apart from a sandy interval (~20 cm core depth), 004PC shows quite uniform clayey silt, with <2% sand from 0 to 400 cm. Sand content increases slightly within the laminated silty clay (400–450 cm) and markedly within the basal diamicton (reaching 55% below 450 cm; Fig. 3). The coarse fraction (>125 μm) also increases towards the base. Sedimentation rates are low within the upper ~400 cm (<0.1 mm/cal yr) but increase towards the core base (max. 45 mm/cal yr). Density (~1–2.5 g/cm^3) is highest in the diamicton. MS measures between −15 and 40×10^{-5} SI, with peaks of ~90×10^{-5} SI near the top (~10 cm) and at the transition from massive to laminated sediments (~393 cm). BioSil generally decreases below 220 cm (Fig. 3).

4.2. Micro- and macro-paleontology

Palynomorphs are generally abundant and well-preserved above the diamicton. Dinocyst concentrations (range 23–27,300 cysts/g; average 8970 cysts/g) and fluxes (range 10–306,000 cysts/cm^2/cal yr; average 112,000 cysts/cm^2/cal yr; Fig. 4a) are lowest in the laminated unit (~400–450 cm) and highest in the uppermost 160 cm massive sediments (Fig. 4a). The sparse dinocysts within the diamicton are likely reworked as indicated by the pre-Late Wisconsinan ages (Table 1). Dinocyst assemblages are primarily composed of *I. minutum* and *Brigantedinium* spp. with lesser *I. cezare* s.l. proportions. *I. minutum* and *Brigantedinium* spp. generally co-dominate Canadian High Arctic surface sediments (Mudie and Rochon, 2001); *Protoperidinium* cysts (possible *Brigantedinium* spp.) are also abundant. *I.? cezare* and *E. karaense* are generally considered faithful indicators of severe sea-ice regimes (Kunz-Pirrung, 1998; Head et al., 2001; Mudie and Rochon, 2001; Matthiessen et al., 2005), though *I.? cezare* has been recorded in temperate latitudes (Pospelova et al., 2004, 2005). Arctic morphotypes of *Polykrikos* (M1, M2), first described from Russian sediments (Kunz-Pirrung, 1998) are prominent towards the base of the massive muds (300–360 cm; Fig. 4a). Overall, dinocyst assemblages primarily encompass typical high-latitude heterotrophs tolerant of large fluctuations in physical parameters (temperature, salinity, sea-ice; Rochon et al., 1999; Mudie and Rochon, 2001; Matthiessen et al., 2005). Assemblages are less diverse than those reported for the low Arctic CAA (Pieńkowski et al., 2011) and Labrador Arctic fjords (Richerol et al., 2012), though they resemble regional CAA records (Mudie and Rochon, 2001; Mudie et al., 2005; Ledu et al., 2010a, 2010b; Pieńkowski et al., 2012). Phototrophs are rare — only *Spiniferites* sp. occurs in low proportions from 116 to 220 cm (Fig. 4a). NPPs are sparse >360 cm (<2700 specimens/g; <27,000 specimens/cm^2/cal yr), but concentrations increase upwards, especially <100 cm, where *H. minor*, Acritarch P, and foraminiferal linings (forms A–E) are abundant (Fig. 4b). Conversely, foraminiferal linings and phytodebris are most abundant between 250 and 80 cm.

Foraminifera are abundant between ~400 and 180 cm (Fig. 5). Sparse foraminifera within the diamicton (>453 cm) are likely reworked given their pre-Late Wisconsinan ages (Table 1). Foraminiferal abundances are especially high at the base of the massive unit (~400–380 cm; Fig. 5), benthics generally outnumbering planktonic foraminifera by an order of magnitude. Although the total foraminiferal fauna likely incorporates smaller (>45 μm) taxa (cf. Schell et al., 2008a, 2008b; Scott et al., 2009), our >125 μm fraction comprises prominent Arctic shelf species, including: *I. norcrossi* and *Cassidulina reniforme*, *Elphidium* sp., *Cibicides lobatulus*, and *Nonionellina labradorica* (Vilks, 1969, 1989; Schröder-Adams et al., 1990; Hunt and Corliss, 1993). Planktonic foraminifera solely comprise *N. pachyderma* (including aberrant, right-coiling forms sensu Darling et al., 2006). Ostracods (mainly *Cyprideis paralatissimum*) co-occur with planktonic foraminifera. Mollusc shells and fragments occur below ~260 cm depth; undifferentiated macro-algal matter is present throughout (Fig. 5).

4.3. Paleoenvironmental zones

Core 004PC was subdivided into seven paleoenvironmental zones based on a combination of litho- and biostratigraphic characteristics. These zones record major environmental changes through time, as shown in both age (cal ka BP; age-depth model derived) and core depth domains (Figs. 3–5).

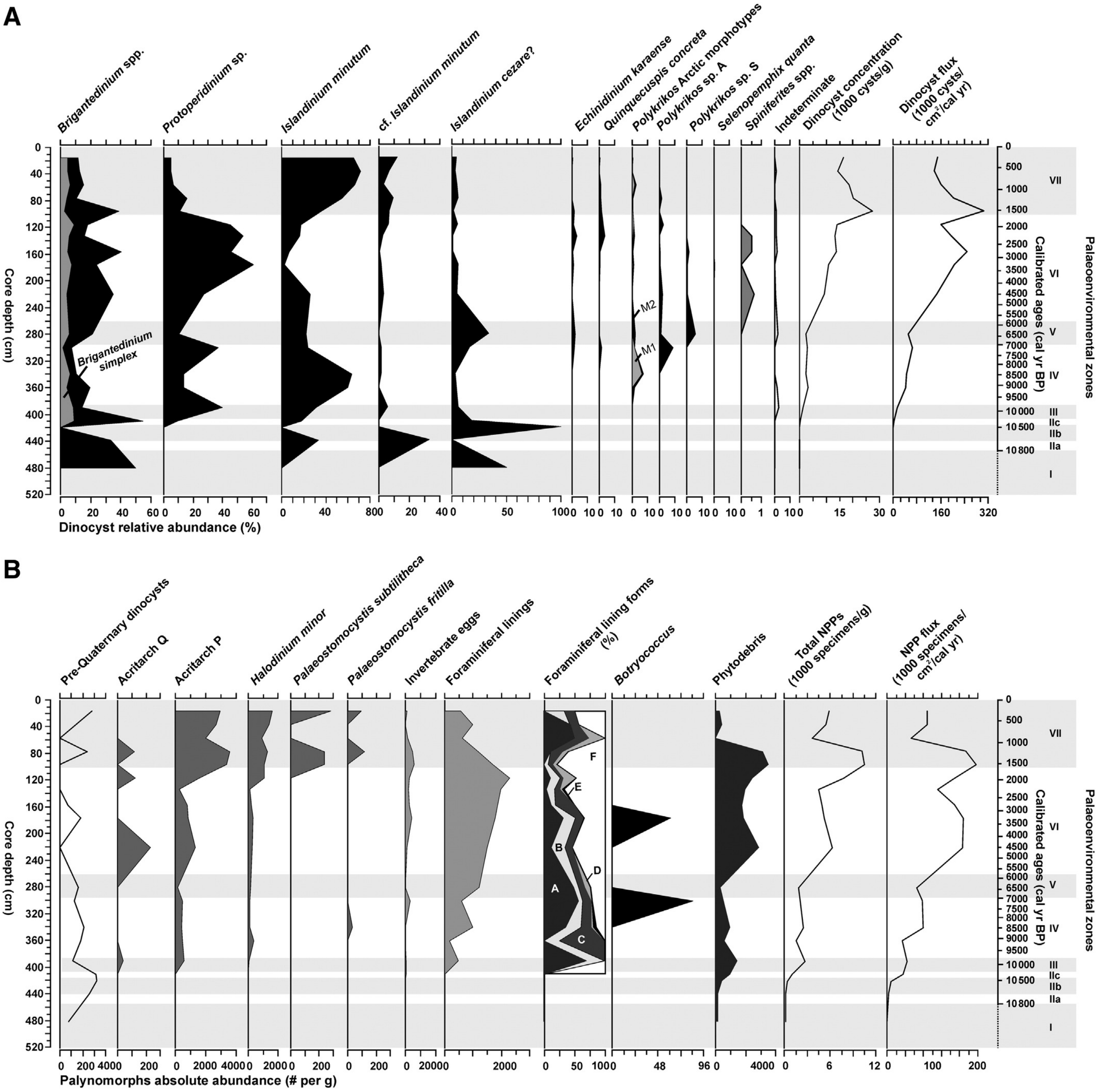

Fig. 4. Results of organic-walled microfossil analyses on core 9722-004PC. (A) Relative (%) and absolute abundances (cysts/dry g sediment), and fluxes (cysts/cm^2/cal yr) of dinoflagellate cysts. (B) Absolute abundances (specimens/g) and fluxes (specimens/cm^2/cal yr) of acritarchs, zoomorphs, freshwater algae, and phytodebris. The relative abundance of foraminiferal lining types sensu Stancliffe (1991) is also shown. The age-depth relationship is given according to the age-depth model (Fig. 2).

4.4. Zone I (523–453 cm; >10.8 cal ka BP)

4.4.1. Chronology

1. Three ^{14}C dates (Table 1) pre-date the LGM, the youngest age being ~40.6 ^{14}C ka BP. Extrapolation of the age-depth model indicates a Zone I/II boundary at ~10.8 cal ka BP (Fig. 2).

4.4.2. Characteristics

The sandy gravelly mud of Zone I, crudely stratified in X-radiography, shows the coarsest sediment, highest density (~2.5 g/cm^3), and highest sedimentation rates (4–45 mm/cal yr) within 004PC. MS (-15.1 to 12.6×10^{-5} SI) and BioSil (2.36%) are relatively low. Sparse microfossils include benthic foraminifera (*C. lobatulus*, *C. reniforme*, *Stetsonia horvathi*) and dinocysts (*Brigantedinium* spp., *I. cezare*); pre-Quaternary dinocyst and phytodebris concentrations are elevated.

4.4.3. Interpretation

Zone I is a diamicton deposited during the last deglaciation. Crude stratification is characteristic of an ice-proximal glaciomarine environment (e.g., “rainout till” sensu Kellogg and Kellogg, 1998; Anderson et al., 1992; Licht et al., 1999) accompanied by decoupling of glacial ice from the seabed. The coarse texture and density – less than typical lodgement till (Kellogg and Kellogg, 1998) – support this interpretation. Similarly, sparse microfossils, abundant pre-Quaternary dinocysts, and pre-Late Wisconsinan molluscs (Table 1) are consistent with glacial

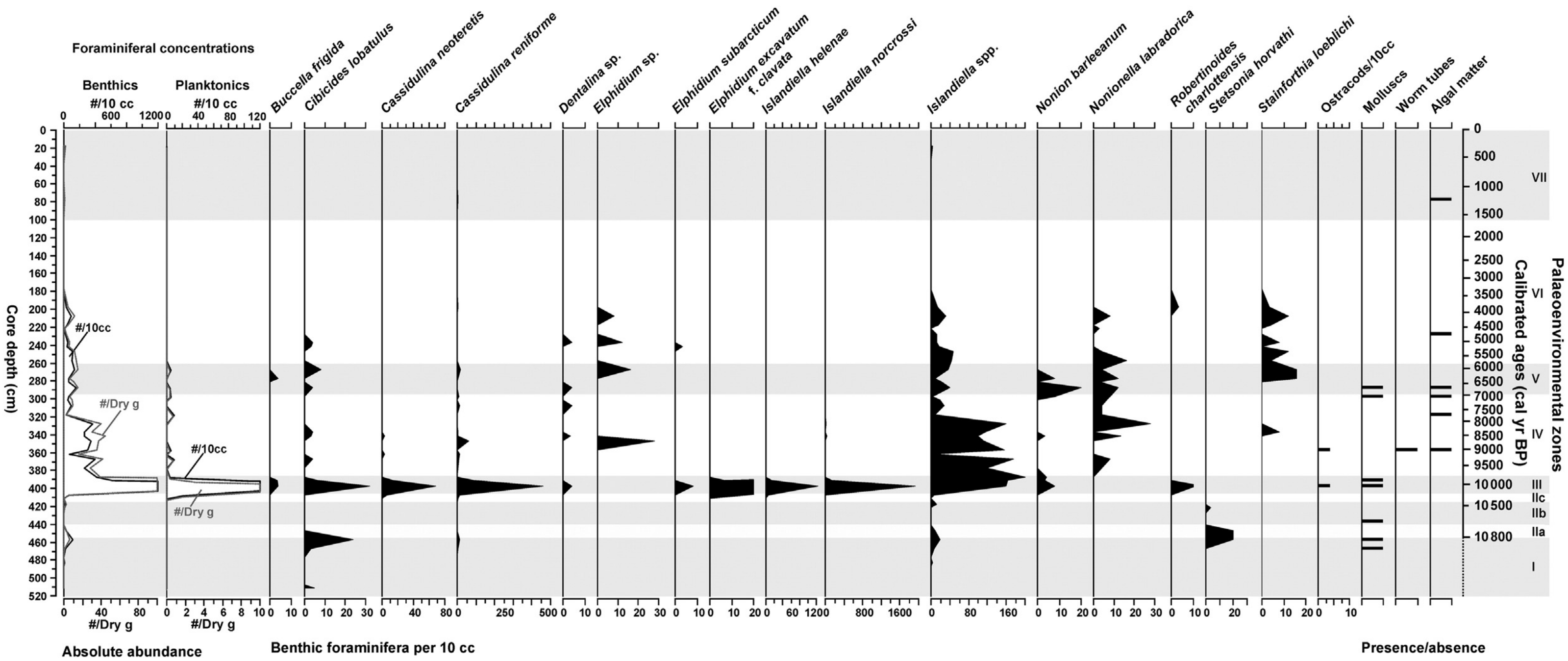

Fig. 5. Results of calcareous microfossils and macrofossils >125 μm in core 9722-004PC. Total absolute abundances of benthic and planktonic foraminifera (solely *Neogloboquadrina pachyderma*) are shown per 10 cc (upper x-axes) and per dry gram (lower x-axes). Absolute abundances of individual benthic foraminiferal taxa and total ostracods are given per 10 cc. Other materials (including molluscs, worm tubes, and macro-algae) are classified according to presence/absence. The age-depth relationship is given according to the age-depth model (Fig. 2).

reworking of older marine sediments. Radiocarbon dates provide a maximum age for local ice advance at ≤40.6 ^{14}C ka BP (Table 1).

4.5. Zone II (453–406 cm; ~10.8–10.3 cal ka BP)

4.5.1. Chronology

In the absence of reliable (non-reworked) dates, age-depth model extrapolation (Section 3.3) indicates the following subzone boundaries: Subzone IIa (453–440 cm, 10.8–10.7 cal ka BP); Subzone IIb (440–416 cm, 10.7–10.4 cal ka BP); Subzone IIc (416–406 cm, 10.4–10.3 cal ka BP; Fig. 2).

4.5.2. Characteristics

Zone II comprises laminated, lonestone bearing, silty clay with slightly higher MS (~−3 to 12×10^{-5} SI), lower bulk density (~1.7 g/cm^3) and increased BioSil (max. 3.68%) than Zone I. Based on litho- and biostratigraphy, three subzones are apparent. Laminated silty clay with lonestones and two sand horizons (Subzone IIa) is overlain by laminated silty clay (Subzone IIb), capped by faintly laminated silty clay with lonestones (Subzone IIc). Foraminiferal and dinocyst abundances increase upwards, but are rare within Subzone IIb. Foraminifera include only benthic taxa (*I. norcrossi*, *C. reniforme*, *Elphidium* sp., *S. horvathi*). Low-diversity dinocyst assemblages of Subzones IIa and IIc are dominated by *Brigantedinium* spp. and *I. minutum* with lesser *Protoperidinium* spp., whereas *I.? cezare* dominates Subzone IIb. Acritarchs and zoomorphs are rare; however, infrequent *H. minor* and invertebrate eggs first appear in Subzone IIc. Phytodebris (max. 960/g) is elevated compared to Zone I, whereas pre-Quaternary dinocysts reach highest concentrations within 004PC (max. 320 specimens/g).

4.5.3. Interpretation

Zone II represents initially ice-proximal to increasingly distal glaciomarine conditions initiated at ~10.8 cal ka BP. Subzone IIa is the most ice-proximal; coarse sediments, including lonestones (interpreted as dropstones) being deposited when ice retreated northward into McDougall Sound. The prominent sandy horizons bounding Subzone IIa are typical of ice-proximal glaciomarine sequences with grounding-line fan and turbidity current deposition (Kellogg and Kellogg, 1998; Evans and Pudsey, 2002). High clastic sediment input limits nutrients and food supply, as reflected in low bioproduction (Korsun and Hald, 1998; Jaeger and Nittrouer, 1999; Gordillo and Aitken, 2001). Prominently-laminated sediments in Subzone IIb indicate cessation of coarse sediment deposition, rapid retreat of glacial ice from the site, and establishment of ice-distal conditions. However, these glacially-influenced laminated sediments qualitatively contain fewer dropstones than usual mid to late Holocene Arctic marine deposits below mobile sea-ice (Pieńkowski et al., 2012). Alternatively, either an ice-shelf marked by basal on-freezing rather than undermelt (Holland et al., 2007), or severe landfast sea-ice that limited dropstone deposition prevailed during Subzone IIb. Similar early Holocene laminated facies are noted for sediments north of Axel Heiberg Island (Hein et al., 1990; Hein and Mudie, 1991). Biological productivity remains low in Subzone IIb, conversely to Subzone IIc: foraminifera and dinocysts are characterized by monospecificity and extremely low concentrations (<160 cysts/g; <36 benthic foraminifera/10 cc). Subzone IIb taxa (*S. horvathi*, *I.? cezare*) can, however, withstand extreme conditions characterized by perennial sea-ice and minimal food (Green, 1960; Wollenburg and Mackensen, 1998; Head et al., 2001; Matthiessen et al., 2005). This agrees with pervasive landfast sea-ice, although it does not preclude an ice-shelf (basal on-freezing) with advection of sparse organic material (Domack and Harris, 1998; cf. Post et al., 2007). Critically, the markedly impoverished microfossil assemblages contradict interpretation of this subzone as an ice-distal environment where rising concentrations and diversities are expected (Korsun and Hald, 1998; Jaeger and Nittrouer, 1999; Gilbert et al., 2002; Knudsen et al., 2008; Pieńkowski et al., 2012).

Recommencing coarse deposition and faint laminae in Subzone IIc mark the return to ice rafting within an ice-distal setting (Evans and Pudsey, 2002). Rising productivity is marked by increasingly abundant and diverse microfossils and elevated BioSil. Similar stratigraphies recording pervasive landfast sea-ice with limited ice-transported detritus (IRD) as in Subzone IIb, followed by a return to dropstone deposition on ice break-up (Subzone IIc), are reported for east Greenland (Dowdeswell et al., 1994a, 1994b, 2000; Ó Cofaigh and Dowdeswell, 2001) and the Axel Heiberg Island continental margin (Hein et al., 1990; Hein and Mudie, 1991).

Overall, highly abundant pre-Quaternary dinocysts and pre-Late Wisconsinan molluscs within Zone II indicate a notable reworked component in the fossil assemblages and reinforce the interpretation of a glacially-influenced, ice-proximal to ice-distal glaciomarine environment.

4.6. Zone III (406–386 cm; 10.3–9.8 cal ka BP)

4.6.1. Chronology

Zone III encompasses two foraminifera-based radiocarbon dates (benthics: OS-92978, 10.4 cal ka BP; planktonic foraminifera: OS-95119, 10.0 cal ka BP; Table 1); two deposit-feeding mollusc dates are excluded due to the Portlandia Effect.

4.6.2. Characteristics

Silty clay, rare small lonestones, relatively fine sediments, and low sedimentation rates (<1 mm/cal yr) characterize Zone III (Fig. 2). Density decreases through this zone (~1.7–1 g/cm^3) whereas MS shows a peak (~93.9×10^{-5} SI), decreasing (~50.3×10^{-5} SI) upwards (Fig. 3). Dinocyst concentrations (>160 cysts/g) and fluxes (>3400 cysts/cm^2/cal yr) are higher than in underlying zones; assemblages include *I. minutum*, along with *Protoperidinium* spp., *Brigantedinium* spp., and *I.? cezare* (Fig. 4). NPP diversity, abundance, and flux increase (>1000 specimens/g; >20,000 specimens/cm^2/cal yr), and acritarchs P and Q, and foraminiferal linings (forms A, B) appear for the first time (Fig. 4). Abundant benthic foraminifera include *I. norcrossi*, *C. reniforme*, *C. lobatulus*, *E. excavatum* f. *clavata*, and *C. neoteretis*; *N. pachyderma* has its maximum abundances within 004PC (Fig. 5). Ostracods (*C. paralatissimum*), molluscs (*Yoldiella fraterna*), and infrequent worm (polychaete?) tubes also occur (Fig. 5).

4.6.3. Interpretation

Zone III represents terminating ice-distal conditions and commencement of massive, fine-grained sedimentation and low sedimentation rates typical of postglacial CAA lithologies (MacLean et al., 1989; Andrews et al., 1991; Pieńkowski et al., 2012). Reduced dropstones (lonestones) suggest less iceberg rafting, with sea-ice as the primary IRD agent. High MS may indicate high iron concentrations, suggesting an extra-local source rather than the calcareous-bedrock-dominated Parry Channel (Thorsteinsson and Kerr, 1967). Closest iron-rich lithologies are on Somerset Island and Boothia Peninsula (Trettin, 1989), implying southerly ice-rafting.

Zone III marks the onset of prominent biological productivity with elevated microfossil diversities and abundances, and increased BioSil (Figs. 3–5). Micro- and macrofossils (worm tubes, molluscs, ostracods) imply increased biological productivity (Fig. 5). Of particular importance is the appearance of planktonic foraminifera, today rare in Parry Channel east of the Lowther–Young sill due to shallow water depths (Vilks, 1974, 1989; Schröder-Adams et al., 1990; Hunt and Corliss, 1993). Planktonic foraminifera suggest significant influx of deeper water (>200 m), most likely AIW, into western Parry Channel. Abundant benthic *Nonion barleeanum* (=*Melonis zaandami*; Schäfer and Cole, 1986) and *C. neoteretis* also mark inflow of saline, relatively warm Atlantic bottom waters within the CAA (cf. Hunt and Corliss, 1993; Jennings et al., 2006, 2011; Pieńkowski et al., 2012).

4.7. Zone IV (386–295 cm; 9.8–7.0 cal ka BP)

4.7.1. Chronology

Three dates on a polychaete tube (OS-74899), algal matter (OS-74915), and mixed benthic foraminifera (MBF; Beta-124622) constrain the age-depth model in Zone IV (Table 1; Fig. 2); three molluscan dates potentially subject to the Portlandia Effect are excluded.

4.7.2. Characteristics

The massive silty clay with infrequent lonestones in Zone IV is similar to that in Zone III (Fig. 2). Density is near-uniform (~1 g/cm^3) whereas MS initially decreases (37.7–3.8 × 10^{-5} SI) before rising slowly up-core (25.1 × 10^{-5} SI). BioSil values are ~4.3%, slightly higher than in Zone III (Fig. 3). Dinocyst concentrations, diversities, and fluxes increase steadily (Fig. 4), with prominent *Brigantedinium* spp. and *I. minutum*, and the first appearance of *Polykrikos* Arctic morphotypes. Abundances of *I.? cezare* s.l. are reduced, and NPP concentrations (*H. minor*, invertebrate eggs, foraminiferal linings A–E) rise whereas foraminiferal abundances decrease (Figs. 4, 5). Foraminiferal diversities are higher than in Zone III; *Islandiella* spp. and *C. reniforme* are now accompanied by *N. labradorica*. Planktonic foraminifera are much reduced; ostracods (*C. paralatissimum*) occur sporadically. Molluscs (*Portlandia arctica*; *Retusa* sp.), worm tubes, and phytodebris are abundant (Fig. 5).

4.7.3. Interpretation

Zone IV represents continued species diversification across all microfossil groups. High Arctic species (e.g. *I. minutum*, *Brigantedinium* spp., *I.? cezare*) are joined by indicators of Atlantic-derived waters, as in Zone III, including *N. pachyderma* (Vilks, 1974, 1989), *N. barleeanum* (Schäfer and Cole, 1986) and *C. neoteretis* (Jennings et al., 2006, 2011). Favorable conditions are also suggested by *N. labradorica*, indicative of heightened phytodetritus influx (Korsun and Hald, 1998; Jennings et al., 2004), and the infaunal *N. barleeanum* which has been linked to highly organic sediments and low oxygen levels (as *M. zaandami*; Mackensen et al., 1985; Schumacher, 2001). Abundant invertebrate eggs and macrofossils imply greater productivity, consistent with elevated BioSil and higher primary production. Occurrence of a carnivorous opisthobranch gastropod (*Retusa* sp.) suggests that the Zone IV ecosystem supported a rich food web, including predators (Thomsen and Vorren, 1986). Reduced coarse sediment input implies cessation of glacially-influenced sedimentation and commencement of postglacial sedimentation similar to modern conditions (MacLean et al., 1989; Pieńkowski et al., 2011, 2012). Nevertheless, infrequent dropstones indicate mobile sea-ice or sporadic icebergs.

4.8. Zone V (295–260 cm; ~7.0–5.8 cal ka BP)

4.8.1. Chronology

One MBF date (Beta-124621; Table 1) is available from the top of this zone.

4.8.2. Characteristics

Lithologically, Zone V is similar to Zone IV (Figs. 2, 3) but the dinocyst assemblage composition differs in having a pronounced *I.? cezare* peak (~33%), elevated *E. karaense* and *Brigantedinium* spp., reduced *I. minutum*, and sparse *Polykrikos* (Fig. 4). NPPs are rare, with only foraminiferal linings increasing (Fig. 4). Total foraminiferal concentrations remain low; *Buccella frigida* and *Elphidium* sp. show small peaks, whereas *N. labradorica* and planktonic foraminifera abundances decline (Fig. 5).

4.8.3. Interpretation

Zone V implies deteriorating environmental conditions. Abundant *I.? cezare* indicates a sea-ice increase, and may record severe (perennial) pack ice (Head et al., 2001; Matthiessen et al., 2005). Along with decreasing microfossil concentrations and diversities, these ice-indicators imply the onset of harsh environmental conditions. This zone marks the last appearance of planktonic foraminifera and some benthic foraminifera (e.g. *N. barleeanum*). Zone V likely represents cessation or reduction of warmer AIW inflow into western Parry Channel and transition to cooler, AOSW-dominated circulation (Zones VI–VII).

4.9. Zone VI (260–100 cm; ~5.8–1.6 cal ka BP)

4.9.1. Chronology

Two dates (MBF, Beta-124620; algal matter, OS-74918) were derived for this zone (Table 1).

4.9.2. Characteristics

Zone VI is texturally identical to Zones IV and V. Density and MS decline slightly upwards, but BioSil increases substantially (from 3.60 to 8.31%). Dinocyst concentrations are three to six times greater than Zone V. *I. minutum* (3–17%) and *I. cezare* show reduced percentages; *Protoperidinium* cysts dominate dinocyst assemblages, while *Polykrikos* spp. and *Spiniferites* spp. occur sporadically. Abundances of *H. minor*, Acritarch P, and foraminiferal linings are elevated. Planktonic foraminifera are absent, while benthic foraminifera are infrequent. Only *I. norcrossi* and rare *N. labradorica*, *Elphidium* sp., and *Stainforthia loeblichi* occur. Ostracods and molluscs are absent, and macro-algal matter occurs sporadically.

4.9.3. Interpretation

Zone VI is considered a progression to 'modern' (i.e. AOSW-influenced) environmental conditions characterized with low salinity and temperature, and prolonged seasonal sea-ice cover. Typical High Arctic taxa (*Brigantedinium* spp., *I. minutum*, *Polykrikos* Arctic morphotypes) occur, though phototrophic dinocysts (*Spiniferites* sp.) suggest seasonally open water (Mudie and Harland, 1996; cf. Matthiessen et al., 2005). However, the marked *I. minutum* reduction is unusual in both modern (Mudie and Rochon, 2001) and paleo-CAA contexts (Ledu et al., 2010a, 2010b; Pieńkowski et al., 2011, 2012), as this prolific taxon generally dominates dinocyst communities. The rise in round brown *Protoperidinium* cysts may be due to out-competing other species for food or alternatively, preservation issues (cf. Zonneveld et al., 2007). Increased BioSil may indicate abundant sea-ice diatoms, a prominent food source for heterotrophic dinoflagellates (e.g. Levinsen and Nielsen, 2002; Sherr and Sherr, 2007). Zone VI marks the disappearance of calcareous benthic foraminiferal tests (≤4.7 cal ka BP), as documented from eastern Parry Channel (Gregory et al., 2010; Pieńkowski et al., 2012).

4.10. Zone VII (100–0 cm; 1.6 to ≤0.75 cal ka BP)

4.10.1. Chronology

One molluscan deposit-feeder ^{14}C date (Table 1; 44 cm; Beta-115388; 870 cal yrs BP) provides a maximum age on age-depth model projection and a core top age of 750 yrs BP, with a minimum core top age of 0 yrs BP. An age closer to 750 yrs BP is more consistent with loss of upper seabed sediments during piston coring.

4.10.2. Characteristics

Aside from a sandy peak towards the top, this zone is texturally identical to Zone IV. Density values are slightly lower (~1.3 g/cm^3) than in Zone VI; shows a pronounced peak (~88.0 × 10^{-5} SI) towards the top, and BioSil reaches maximum values (12.31%). Palynomorph concentrations and fluxes show maxima (27,300 cysts/g; 10,500 NPPs/g; 306,000 cysts/cm^2/cal yr; 118,000 NPPs/cm^2/cal yr). Dinocyst assemblage structures are similar to modern assemblages: *I. minutum* and *Brigantedinium* spp. co-dominate, while *I.? cezare* and *Polykrikos* spp.

are reduced. NPP Acritarch P, *P. subtilitheca*, and *P. fritilla* have peak concentrations, but foraminiferal linings decline, in accordance with decreasing foraminiferal tests.

4.10.3. Interpretation

Zone VII represents essentially modern environmental conditions of 10 month sea-ice cover per year and AOSW throughflow in McDougall Sound. The MS peak in the sandy layer may reflect either enhanced sea-ice rafting due to an increase in volume, mobility, or melt-out (Smith and Andrews, 2000; Ó Cofaigh and Dowdeswell, 2001; Andrews et al., 2002), or sporadic icebergs entering the area. Dinocyst assemblages are typical of the central CAA (Mudie and Rochon, 2001; Ledu et al., 2010a, 2010b). NPP assemblages are similar to cold water communities from Greenland and Coronation Gulf (Mudie and Harland, 1996; Roncaglia, 2004; Roncaglia and Kuijpers, 2004; Pieńkowski et al., 2011, 2012). The sparsity of >125 μm calcareous benthic foraminifera is typical of modern CAA conditions (Gregory et al., 2010; von Prause, 2011; Pieńkowski et al., 2012), in contrast to the Canadian Polar Margin (Schröder-Adams et al., 1990). Although foraminiferal linings decline, their presence throughout Zone VII suggests the occurrence of foraminifera not found as microfossils >125 μm. Such disappearance may be due to taphonomic (dissolution, destruction of delicate agglutinates due to oven-drying) and/or biological (switch to smaller and/or delicate agglutinates) factors (cf. Furze et al., 2010).

5. Discussion

5.1. Immediate deglaciation (>10.8 cal ka BP)

The crudely stratified Zone I unit provides the first documentation of the deglacial chronology of the central CAA marine channels and expands upon pre-existing, adjacent land-based records. Zone I density values are similar to marine diamictons in eastern Parry Channel (MacLean et al., 1989). Lodgement till deposited by grounded LGM ice potentially underlies such units, however its high bulk densities and shear strengths (Anderson et al., 1992; Licht et al., 1996) inhibit core penetration. Contrary to earlier models proposing LGM ice-shelves (Dyke and Prest, 1987), grounded ice is now invoked for Viscount Melville Sound (England et al., 2009), Peel Sound and Prince Regent Inlet (MacLean et al., 2010), and other CAA straits (Blasco et al., 2005). This paper builds on this consensus.

Reworked pre-Late Wisconsinan dates within Zone I provide a maximum limiting age (39.8 ^{14}C ka BP) on initial ice advance through the marine channels of the central CAA. This date is comparable with other age determinations from till on Griffith (~41 ^{14}C ka BP) and Cornwallis islands (~27.3–36.5 ^{14}C ka BP, Washburn and Stuiver, 1985). Understandably, these dates do not constrain timing of ice-sheet float-off and breakup. Extrapolation of the 004PC age-depth model below the lowermost reliable date (Section 3.2) indicates that deglaciation occurred at ~10.8 cal ka BP. An LGM Laurentide trunk glacier (*not* Innuitian ice) occupied Lowther, Griffith and (possibly) southern Bathurst and Cornwallis islands, while a radially-flowing local ice cap occupied the Devon Island coast until 10.4 cal ka BP (9.5 ^{14}C ka BP, Dyke, 1993). Striations on Lowther Island suggest the persistence of at least a residual local ice cap until ≥10.4 cal ka BP (Dyke, 1993), implying limited Innuitian ice drainage south through McDougall Sound at this time. Nonetheless, the configuration of McDougall Sound would have favored maintenance of grounded ice later than in western Barrow Strait, as evidenced by a 10.0 cal ka BP deglacial date from nearby Truro Island (9.2 ^{14}C ka BP, Washburn and Stuiver, 1985; Fig. 1).

We recognize that our current deglacial chronology is complicated by the uncertainty of an enhanced deglacial ΔR (Hanslik et al., 2010), sparse dateable materials (e.g., Pieńkowski et al., 2012), and the Portlandia Effect (Coulthard et al., 2011; England et al., 2012). These factors challenge the assumption that marine cores in this part of the CAA can yield meaningful "basal ages" permitting precise determination of deglacial timing at this site.

5.2. Ice-proximal to ice-distal progression (~10.8–10.3 cal ka BP)

Zone II records succession from ice-proximal (Zone IIa) to ice-distal (Zone IIc) conditions. Laminated silty clay with coarse sand and dropstones (Zone IIa) typical of the early deglacial NWP (MacLean et al., 1989; Mudie et al., 2006; Pieńkowski et al., 2012) signifies close proximity to the glacial grounding line. The subsequent dropstone-free, well laminated sediments (Zone IIb) may record deposition from an ice-shelf or an interval of severe sea-ice following deglaciation, as reported from southeastern Barrow Strait (Pieńkowski et al., 2012) and eastern Greenland (Scorsby Sund; Dowdeswell et al., 1994a, 1994b, 2000; Ó Cofaigh and Dowdeswell, 2001). Lithostratigraphically, distinguishing between ice-shelf vs. perennial sea-ice deposition (e.g., Zone IIb) is highly problematic, both settings producing similar sediments under conditions of basal on-freezing (Holland et al., 2007). Nevertheless, limited potential for deglacial basal on-freezing, coupled with greater glacio-isostatic water depths (Dyke et al., 1991) and higher tidal amplitudes (Griffiths and Peltier, 2008) during this interval argue against a cohesive glacially-fed ice-shelf in western Barrow Strait for which no sedimentological or geomorphic evidence has been reported. On the basis of the current evidence for an abrupt lift-off of the formerly grounded trunk-glacier, we interpret the absence of lithic material >250 μm in Zone IIb as evidence of pervasive landfast sea-ice as found in deglacial Parry Channel (Pieńkowski et al., 2012, submitted for publication). The overlying faintly laminated sediments with dropstones (Zone IIc) likely indicate increasing distance from the grounding line following sea-ice break-up (Zone IIb; Cowan et al., 1997; Gilbert et al., 2002).

Zone II represents increasingly favorable conditions for bioproduction, expressed as rising microfossil abundance and diversity, and rising BioSil, similar to other CAA glaciomarine settings (Pieńkowski et al., 2012). Previous, qualitative foraminiferal data from 004PC glaciomarine sediments (Blasco et al., 2005) were interpreted as an 'ice-shelf' community. However, succession across all microfossil groups and increasing BioSil (diatoms) suggest increasingly ice-distal conditions rather than presence and break-up of an ice-shelf (Post et al., 2007).

5.3. Deep-water penetration (~10.3–9.8 cal ka BP)

Zone III marks the commencement of deposition of massive fine-grained, bioturbated sediments with infrequent dropstones typical of the Holocene CAA (MacLean et al., 1989; Andrews et al., 1991; Pieńkowski et al., 2012). Simultaneously, this represents the start of higher bioproductivity including planktonic and benthic microbiota, polychaetes, crustaceans, and molluscs. Of particular significance is the appearance of planktonic foraminifera (*N. pachyderma*) soon after deglaciation, peaking at ~10.0 cal ka BP (Fig. 6), as found in eastern Parry Channel (cf. Vare et al., 2009; cf. Gregory et al., 2010; Pieńkowski et al., 2012). Planktonic foraminifera are rare in the modern central CAA due to shallow water depths and the restricted, sill-controlled circulation (Vilks, 1969, 1974, 1989; Hunt and Corliss, 1993). However, deglacial water depths were greater due to glacio-isostatic depression (Dyke et al., 1991; England et al., 2006). Regional marine limit is ~125 m (Dyke et al., 1991) above modern sea-level, implying deglacial water depths of ~390 m at the core site (modern water depth 267 m). Such physiography would significantly alter CAA oceanography, allowing for penetration of deeper waters carrying planktonic foraminifera, such as AIW below ~250 m (Jones and Coote, 1980; Tang et al., 2004). The flow trajectory of this water and the general oceanographic circulation upon deglaciation remain cryptic, however. Following significant deglacial freshwater export, marine mammal (*B. mysticetus*) and molluscan-

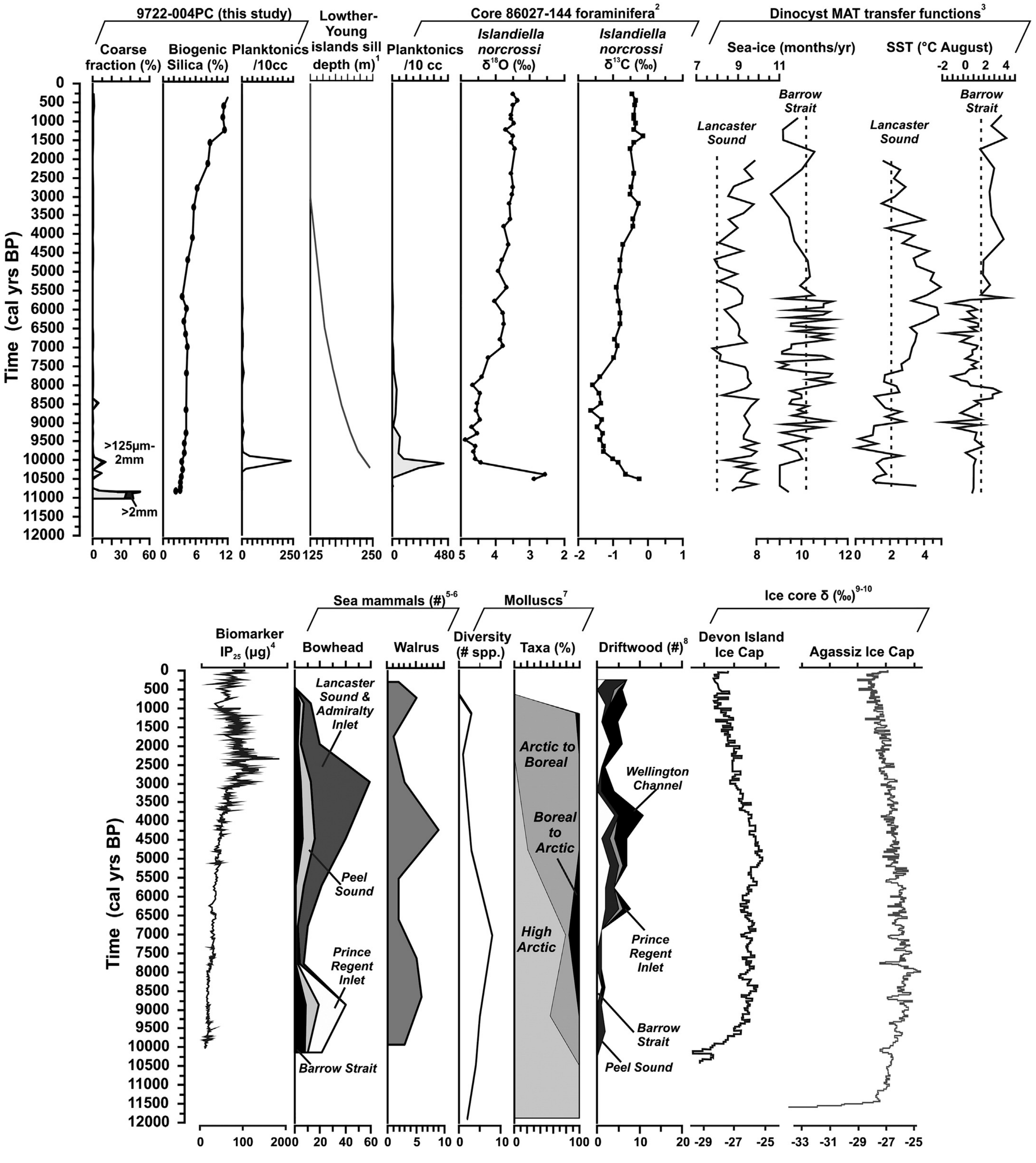

Fig. 6. Comparison between the present study (9722-004PC) and regional data derived from marine and terrestrial environments, including: foraminiferal assemblages and stable isotope ratios, dinocyst-based modern analogue technique (MAT) transfer function reconstructions of sea-surface temperature (SST) and sea-ice (dashed lines denote modern values); mono-unsaturated highly-branched isoprenoids (IP_{25}) from Barrow Strait; marine mammal and driftwood abundances from raised marine shorelines; and ice-core records from Ellesmere (Agassiz Ice Cap) and Devon islands. Water depths at the Lowther–Young islands sill are also shown. Reference designations are as follows: 1: Dyke et al. (1991); 2: Pieńkowski et al. (2012); 3: Ledu et al. (2010a); 4: Vare et al. (2009); 5: Dyke et al., 1996b; 6: Dyke et al., 1999; 7: Gordillo and Aitken (2001); 8: Dyke et al. (1997); 9: Paterson et al. (1977); 10: Fisher et al. (1995). All chronologies are presented as calibrated years BP, and originally uncalibrated dates (Dyke et al., 1991, 1996b, 1997, 1999; Gordillo and Aitken, 2001) were calibrated where necessary.

based reconstructions suggest near-modern surface circulation as early as ~10 cal ka BP, (cf. Andrews et al., 1993; Dyke et al., 1996a, 1996b). If the early Holocene planktonic foraminifera in eastern Parry Channel (Pieńkowski et al., 2012) indicate Baffin Bay-derived AIW, a different circulation to modern would be invoked. Alternatively, a near-modern paleocirculation would suggest a northwest AIW source via Viscount

Melville Sound though deglacial water depths at the Lowther–Young sill (~260 m; Fig. 6) may have been insufficient to allow westward deep water (>250 m) penetration while Queen's Channel (Qu. Ch.; Fig. 1A) may have also been too shallow. More work around the critical Lowther–Young sill is needed to trace the pathway of this prominent planktonic foraminifera signal.

The core site is at the northern end of the Lowther–Young sill, the postulated location for final decoupling of Laurentide and Innuitian ice-sheets (Dyke, 2004) and the establishment of oceanic throughflow via Parry Channel (Dyke et al., 1996b; Pieńkowski et al., 2012). Deglacial dates for Lowther Island (Dyke, 1993) and the 004PC site (this study) constrain the timing of final Innuitian and Laurentide separation to between 10.8 and 10.4 cal ka BP. Given the first appearance of planktonic foraminifera in 004PC, the initiation of marine transport across the Lowther–Young sill is tentatively assigned (age-depth model extrapolation) to ~10.3 cal ka BP.

5.4. Biologically favorable conditions (~9.8–7.0 cal ka BP)

Following the influx of planktonic foraminifera into central Parry Channel, all fossil groups show increased diversity and abundances, accompanied by increased BioSil. Higher organisms such as molluscs (including gastropods) also occur, suggesting a productive ecosystem at both benthic and planktonic levels and more favorable environmental conditions.

An amelioration, following the early Holocene planktonic foraminifera signal, is also apparent in eastern Parry Channel (Pieńkowski et al., 2012), and has been linked to a regional Holocene Thermal Maximum (HTM; Kaufman et al., 2004 vs. Gajewski et al., 2000), itself potentially promoted by maximum solar radiation receipts (Tricot and Berger, 1988; Bradley, 1990). In the study area, Kaufman et al. (2004) proposed HTM commencement at 10.0–8.0 cal ka BP and termination by 5.0–6.0 cal ka BP. Zone IV may encompass this amelioration, but dinocyst assemblages differ compared to eastern records. Specifically, cysts of obligate phototrophs (*Operculodinium centrocarpum*, *Spiniferites elongatus*), present during this time in eastern Parry Channel and interpreted to indicate extended summer open water (Pieńkowski et al., 2012), are absent in 004PC. Reduced sea-ice >6 cal ka BP is also proposed by IP_{25} (mono-unsaturated highly branched isoprenoids from sea-ice diatoms) from southeastern Barrow Strait and the southwestern CAA (Vare et al., 2009; Belt et al., 2010). Not all interpretations agree with a regional marine amelioration at the time, however. In particular, quantitative dinocyst transfer functions based on modern analogue techniques (MAT) from Barrow Strait show highly fluctuating, though cooler conditions 8–5 cal ka BP, similar to MAT reconstructions from Lancaster Sound (Fig. 6; Ledu et al., 2008, 2010a).

Nonetheless, data from adjacent islands support a thriving ecosystem during an ameliorated early to mid Holocene (Fig. 6), as suggested by micro- and macro-fossils in Zone IV. These data include pollen assemblages from Somerset Island (Gajewski, 1995), maximum melt >6.7 cal ka BP on the Agassiz Ice Cap (Ellesmere Island; Fisher and Koerner, 2003), and range expansions of plants and animals adapted to more favorable environments (Bradley, 1990). Furthermore, marine materials collected from central CAA paleoshorelines suggest a warmer early to mid Holocene with extensive summer open water (Fig. 6), including diverse mollusc assemblages (Dyke et al., 1996a; Gordillo and Aitken, 2001) and reduced driftwood abundances (presumed transported into the CAA by sea-ice; Dyke et al., 1997). Early Holocene (10.2–8.9 cal ka BP; Dyke et al., 1996b) bowhead whale bone abundances coincide with favorable Zone IV conditions, although the later (8.9–5.5 cal ka BP) decline in whale bones attributed to severe sea-ice conflicts with our data and other recent CAA marine records (Vare et al., 2009; Belt et al., 2010; Pieńkowski et al., 2012).

5.5. Development of 'modern' oceanographic conditions (post 7.0 cal ka BP)

Data from 004PC show a mid to late Holocene establishment of essentially 'modern' conditions with minor sea-ice fluctuations (increase 7.0–6.0 cal ka BP; decrease ~5.0–2.0 cal ka BP) whereas the most pronounced environmental changes are evident in the early to mid Holocene. Exclusion of AIW due to glacio-isostatic rebound, coupled with cooling climate (Bradley, 1990; Koerner and Fisher, 1990, 2002; Fisher et al., 1995) likely contributed to the establishment of such 'modern' conditions. Water depth changes explain the disappearance of planktonic foraminifera by 6.0 cal ka BP. By 6.5 cal ka BP, water depths were only ~30 m deeper than present, marking significant postglacial shallowing (+125 m; Fig. 6; Dyke et al., 1991) which restricted water flow to AOSW. Consequently, colder conditions would be expected. The post mid-Holocene progression to near-modern conditions is especially evident in the palynomorph assemblages <2.0 cal ka BP when modern dinocyst assemblages and Arctic acritarchs appear (Mudie and Rochon, 2001; Roncaglia, 2004).

The late Holocene sparsity of benthic foraminifera is typical of CAA sediments (MacLean et al., 1989; Gregory et al., 2010; Pieńkowski et al., 2011, 2012), perhaps due to dissolution and/or switch to smaller/agglutinated taxa (cf. Furze et al., 2010). The >125 μm fraction assessed in this study does not sample smaller taxa and oven-drying may have destroyed the relatively delicate agglutinates (Lloyd et al., 2007). However, agglutinates dominating 004PC sediments <6 cal ka BP were interpreted to indicate AOSW throughflow in a previous (>63 μm) assessment (Blasco et al., 2005), in-keeping with our interpretation of 'modern' oceanography. Our late Holocene foraminiferal concentrations are comparable to regional modern >150 μm data (Hunt and Corliss, 1993), and apparent contradictions (calcareous vs. agglutinated foraminiferal ratios) between our and previous studies may reflect analyzed size fractions [Schröder-Adams et al., 1990 (>63 μm) vs. Hunt and Corliss, 1993 (>150 μm)]. Arctic marine records (Mudie et al., 2006; Ledu et al., 2010a; Pieńkowski et al., 2011, 2012; this study) show consistently present foraminiferal linings, even in the absence of calcareous tests, perhaps highlighting the paleoenvironmental potential of foraminiferal linings (von Prause, 2011).

In-keeping with our interpretation of a mid to late Holocene switch to AOSW-dominated circulation, cooler conditions after ~6.0 cal ka BP are also apparent in eastern Parry Channel in IP_{25} and multiproxy marine records (Fig. 6; Short et al., 1994; Vare et al., 2009; Pieńkowski et al., 2012). Notably, the prominent BioSil rise in 004PC after ~7.0 cal ka BP mimics the trend of Holocene IP_{25} elsewhere in the CAA (Fig. 6; Vare et al., 2009; Belt et al., 2010), perhaps corresponding to increased sea-ice diatoms in the regional algal community (Riedel et al., 2003). However, this interpretation requires validation by direct comparison between diatom assemblages, BioSil, and IP_{25}. Contrary to this study and other marine data outlined above, dinocyst MAT transfer functions indicate warming (higher sea-surface temperatures, but longer sea-ice season, compared to modern) in Barrow Strait after 5 cal ka BP (Fig. 6; Ledu et al., 2010a), but with longer sea-ice cover and higher sea-surface temperatures <5 cal ka BP in Dease Strait and Lancaster Sound (Fig. 6; Ledu et al., 2008, 2010a).

Unlike dinocyst transfer functions, terrestrial data support a mid Holocene cooling (Fig. 6). For example, ice cores indicate pronounced cooling <5.5 cal ka BP on Ellesmere Island (Fisher et al., 1995), and <4 cal ka BP on Devon Island (Paterson et al., 1977). Furthermore, increasing driftwood and walrus bone abundances suggest greater sea-ice influence in the central CAA (Fig. 6; Dyke et al., 1997, 1999), as do reduced-diversity paleo-mollusc assemblages, and decreasing boreal-Arctic molluscan taxa after ~6 cal ka BP (Dyke et al., 1996a; Gordillo and Aitken, 2001). Nevertheless, abundant mid to late Holocene (5–3 ^{14}C ka BP ≈ 5.1–2.4 cal ka BP; Fig. 6) bowhead bones previously interpreted as signalling reduced sea-ice (Dyke et al., 1996b) are at odds with regional cooling. However, the highly mobile and migratory life-habit of bowheads, coupled with taphonomic factors (carcass floating/ice-rafting; stranding/ice-trapping locations) likely complicates a straightforward correlation between sea-ice and fossil whale occurrences (Furze et al., submitted for publication).

Although some late Holocene variations are apparent, short-term climatic variations (Little Ice Age, 20th Century warming) are absent in 004PC, similar to other east-central records (Ledu et al., 2008, 2010a; Pieńkowski et al., 2012). This is likely due to: low resolution and low sedimentation rates with high bioturbation; sample site within a zone of high-volume water transport; the High Arctic setting; or primarily dinocyst-based paleoenvironmental interpretations (with invariable late Holocene sediments, apparent disappearance of foraminifera, and cryptic NPPs). Conversely, such episodes are apparent in lacustrine records (e.g., Gajewski and Atkinson, 2003; Smol et al., 2005; Peros and Gajewski, 2009), ice cores (Paterson et al., 1977) and recent marine data from the southwestern CAA and adjacent Beaufort Shelf (Schell et al., 2008b; Pieńkowski et al., 2011; Bringué and Rochon, 2012).

To conclude, the long-term paleoenvironmental histories derived from 004PC agree with many other marine and terrestrial interpretations from the CAA. Notable exceptions are bowhead whale-based interpretations (Dyke et al., 1996b, but see Furze et al., submitted for publication) and dinocyst MAT-based transfer functions (Ledu et al., 2010a, 2010b). Nevertheless, our data as well as other marine and terrestrial CAA archives (e.g., Bradley, 1990; Dyke et al., 1996a; Vare et al., 2009; Pieńkowski et al., 2012) indicate pronounced deglacial to mid Holocene environmental changes fluctuating on a scale not observed today. Discrepancies between this and other marine reconstructions may be attributable to chronostratigraphic factors (ΔR, age-depth model), quantitative vs. qualitative, and single- vs. multiproxy approaches.

Core 004PC offers important new insights on the late Quaternary environmental evolution of the CAA, showing striking similarities to other deglacial to Holocene archives (Pieńkowski et al., 2012). More detailed late Pleistocene–Holocene multiproxy marine records are needed to assess how typical such paleoenvironments are for the CAA in particular, and for Arctic Canada overall. Such records will resolve issues that currently hinder an integrated understanding of CAA paleoceanography, including: deglacial timing and style; sources of early Holocene planktonic foraminifera; and problems within commonly-applied proxy groups (periodically absent foraminifera; low-diversity, invariable dinocysts; cryptic environmental preferences of NPPs). Meanwhile, 004PC constitutes a key link between existing eastern CAA studies and future research into the western CAA, including Viscount Melville Sound and M'Clure Strait.

6. Conclusions

The following conclusions can be drawn from multiproxy analyses on 9722-004PC:

- The basal stratified diamicton (Zone I) interpreted as waterlain 'rain-out till' evidences the last stages of regional deglaciation. Precise deglacial timing is ill-defined due to scarcity of dateable materials at the diamicton/laminated unit transition. Reworked materials of pre-Late Wisconsinan age provide a maximum control on glaciation at 39.8 ^{14}C ka BP. Age-depth model extrapolations suggest deglaciation at ~10.8 cal ka BP.
- Zone II (~10.8–10.3 cal ka BP) shows initially ice-proximal, coarse deposition (IIa), followed by a well-laminated unit (IIb) with sparse microfossils interpreted as a cessation in coarse deposition due to pervasive sea-ice. Returning coarse deposition (IIc) marks increasingly ice-distal conditions with increased biological productivity.
- *N. pachyderma* signal AIW (>250 m depth) penetration either from Baffin Bay or the (north)west Arctic Ocean (Zone III; ~10.3–9.8 cal ka BP). Oceanic throughflow and separation of Laurentide and Innuitian ice sheets are implied by ~10.3 cal ka BP.
- Increasing microfossil abundance and species diversification show ameliorated, biologically favorable conditions at ~9.8–7.0 cal ka BP (Zone IV).
- Polar conditions commence <7.0 cal ka BP (Zones V–VII); near-modern dinocyst assemblages and reduced foraminifera collectively mark AOSW-dominated throughflow.

Acknowledgments

Funding from the NSERC Northern Chair Program awarded to England enabled this research. A MacEwan University Faculty Research, Scholarly Activity and Creative Achievements Fund awarded to Furze, Pieńkowski, England, Blasco, and MacLean ("Deglacial Environments of the Western Canadian High Arctic") is gratefully acknowledged. We thank Charlie Schweger and Harvey Friebe (University of Alberta) for enabling access to their palynology laboratory. We are particularly grateful to Kate Jarrett for core subsampling, and to Owen Brown (both GSC-Atlantic) for conducting grain size analyses. Maureen Soon at the Pacific Centre for Isotopic and Geochemical Research (University of British Columbia) is thanked for BioSil measurements and help with data interpretation. We thank Vera Pospelova, André Rochon, and one anonymous reviewer whose comments improved the manuscript. Geert de Lange is thanked for editorial handling of this manuscript.

References

ACIA, 2005. Arctic Climate Impact Assessment. Cambridge University Press, Cambridge (1042 pp.).

Anderson, J.B., Shipp, S.S., Bartek, L.R., Reid, D.E., 1992. Evidence for a grounded ice sheet on the Ross Sea continental shelf during the late Pleistocene and preliminary paleodrainage reconstruction. Antarctic Research Series 57, 39–62.

Andrews, J.T., Jennings, A.E., MacLean, B., Mudie, P.J., Praeg, D., Vilks, G., 1991. The surficial geology of the Canadian eastern Arctic and Polar continental shelves. Continental Shelf Research 11, 791–819.

Andrews, J.T., Dyke, A.S., Tedesco, K., White, J.W., 1993. Meltwater along the Arctic margin of the Laurentide Ice Sheet (8–12 ka BP): stable isotopic evidence and implications for past salinity anomalies. Geology 21, 881–884.

Andrews, J.T., Kihl, R., Kristjansdottir, G.B., Smith, L.M., Helgadottir, G., Geirsdottir, A., Jennings, A.E., 2002. Holoocene sediment properties of the East Greenland and Iceland continental shelves bordering Denmark Strait (64–68°N), North Atlantic. Sedimentology 49, 5–24.

Barry, R.G., 1993. Canada's cold seas. In: French, H.M., Slaymaker, O. (Eds.), Canada's Cold Environments. McGill-Queen's University Press, Montréal and Kingston, pp. 29–61.

Bednarski, J.M., 2003. Deglaciation of Bathurst Island Group, Nunavut. Geological Survey of Canada, Map 2020A, scale 1:250 000.

Belt, S.T., Vare, L.L., Massé, G., Manners, H.R., Price, A.C., MacLachlan, S.E., Andrews, J.T., Schmidt, S., 2010. Striking similarities in temporal changes to spring sea ice occurrence across the central Canadian Arctic Archipelago over the last 7000 years. Quaternary Science Reviews 29, 3489–3504.

Blasco, S., MacLean, B., Mudie, P., Sonnichsen, G., Bennett, R., Rainey, W., Scott, D., Praeg, D., Hughes-Clarke, J., Bartlett, J., Mayer, L., Monahan, D., 2005. Northwest Passage marine sediments: a record of Quaternary history and climate change. 35th Annual International Arctic Workshop Program and Abstracts 2005. Canadian Circumpolar Institute, University of Alberta, Edmonton, p. 63.

Bradley, R.S., 1990. Holocene paleoclimatology of the Queen Elizabeth Islands, Canadian High Arctic. Quaternary Science Reviews 9, 365–384.

Bradley, R.S., England, J.H., 2008. The Younger Dryas and the Sea of Ancient Ice. Quaternary Research 70, 1–10.

Bringué, M., Rochon, A., 2012. Late Holocene paleoceanography and climate variability over the Mackenzie Slope (Beaufort Sea, Canadian Arctic). Marine Geology 291–294, 83–96.

Coote, A.R., Jones, E.P., 1982. Nutrient distributions and their relationships to water masses in Baffin Bay. Canadian Journal of Fisheries and Aquatic Sciences 39, 1210–1214.

Coulthard, R.D., Furze, M.F.A., Pieńkowski, A.J., Nixon, F.C., England, J., 2010. New marine ΔR values for Arctic Canada. Quaternary Geochronology 5, 419–434.

Coulthard, R.D., Furze, M.F.A., Pieńkowski, A.J., Nixon, F.C., England, J., 2011. The complexity of marine ^{14}C chronologies in Arctic Canada: variable ΔR values, enhanced deep water reservoirs, and the Portlandia effect. Talk presented at the XVIII INQUA Congresss, Bern, Switzerland, 21–27 July 2011.

Cowan, E.A., Cai, J., Powell, R.D., Clark, J.D., Pitcher, J.N., 1997. Temperate glacimarine varves: an example from Disenchantment Bay, southern Alaska. Journal of Sedimentary Research 67, 536–549.

Darling, K.F., Kucera, M., Kroon, D., Wade, C.M., 2006. A resolution for the coiling direction paradox in *Neogloboquadrina pachyderma*. Paleoceanography 21, A2011.

de Vernal, A., Goyette, C., Rodriguez, C.G., 1989. Contribution palynostratigraphique (dinokystes, pollen et spores) à la connaisance de la mer de Champlain: coupe de Saint-Césaire, Québec. Canadian Journal of Earth Sciences 26, 2450–2464.

Domack, E.W., Harris, P.T., 1998. A new depositional model for ice shelves, based upon sediment cores from the Ross Sea and the MacRobertson shelf, Antarctica. Annals of Glaciology 27, 281–284.

Dowdeswell, J.A., Uenzelmann-Neben, G., Whittington, R.J., Marienfeld, P., 1994a. The Late Quaternary sedimentary record in Scoresby Sund, East Greenland. Boreas 23, 294–310.

Dowdeswell, J.A., Whittington, R.J., Marienfeld, P., 1994b. The origin of massive diamicton facies by iceberg rafting and scouring, Scoresby Sund, East Greenland. Sedimentology 41, 21–35.

Dowdeswell, J.A., Whittington, R.J., Jennings, A.E., Andrews, J.T., Mackensen, A., Marienfeld, P., 2000. An origin for laminated glacimarine sediments through sea-ice build-up and suppressed iceberg rafting. Sedimentology 47, 557–576.

Dyke, A.S., 1987. A reinterpretation of glacial and marine limits around the northwestern Laurentide Ice Sheet. Canadian Journal of Earth Sciences 24, 591–601.

Dyke, A.S., 1993. Glacial and sea level histories of Lowther and Griffith islands, Northwest Territories: a hint of tectonics. Géographie Physique et Quaternaire 47, 133–145.

Dyke, A.S., 1999. Last Glacial Maximum and deglaciation of Devon Island, Arctic Canada: support for an Innuitian Ice Sheet. Quaternary Science Reviews 18, 393–420.

Dyke, A.S., 2004. An outline of North American deglaciation with emphasis on central and northern Canada. In: Ehlers, J., Gibbard, P.L. (Eds.), Quaternary Glaciations, Extent and Chronology. Part II. North America. : Development in Quaternary Science, vol. 2b. Elsevier, Amsterdam, pp. 371–406.

Dyke, A.S., Prest, V., 1987. Late Wisconsinan and Holocene history of the Laurentide Ice Sheet. Géographie Physique et Quaternaire XL1 (2), 237–263.

Dyke, A.S., Morris, T.F., Green, D.E.C., 1991. Postglacial tectonic and sea level history of the central Canadian Arctic. Geological Survey of Canada Bulletin 397, 1–56.

Dyke, A.S., Dale, J.E., McNeely, R.N., 1996a. Marine molluscs as indicators of environmental change in glaciated North America and Greenland during the last 18,000 years. Géographie Physique et Quaternaire 50, 125–184.

Dyke, A.S., Hooper, J., Savelle, J.M., 1996b. A history of sea ice in the Canadian Arctic Archipelago based on postglacial remains of the bowhead whale (*Balaena mysticetus*). Arctic 49, 235–255.

Dyke, A.S., England, J., Reimnitz, E., Jetté, H., 1997. Changes in driftwood delivery to the Canadian Arctic Archipelago: the hypothesis of postglacial oscillations of the Transpolar Drift. Arctic 50, 1–16.

Dyke, A.S., Hooper, J., Harrington, C.R., Savelle, J.M., 1999. The Late Wisconsinan and Holocene record of walrus (*Odobenus rosmarus*) from North America: a review with new data from Arctic and Atlantic Canada. Arctic 52, 160–181.

England, J., Atkinson, N., Bednarski, J., Dyke, A.S., Hodgson, D.A., Ó Cofaigh, C., 2006. The Innuitian Ice Sheet: configuration, dynamics and chronology. Quaternary Science Reviews 25, 689–703.

England, J.H., Lakeman, T.R., Lemmen, D.S., Bednarski, J.M., Stewart, T.G., Evans, D.J.A., 2008. A millennial-scale record of Arctic Ocean sea ice variability and the demise of the Ellesmere Island ice shelves. Geophysical Research Letters 35, L19502. http://dx.doi.org/10.1029/2008GL034470.

England, J., Furze, M.F.A., Doupé, J.P., 2009. Revision of the NW Laurentide Ice Sheet: implications for paleoclimate, the northeast extremity of Beringia, and Arctic Ocean sedimentation. Quaternary Science Reviews 28, 1573–1596.

England, J., Dyke, A.S., Coulthard, R.D., Mcneely, R., Aitken, A., 2012. The exaggerated radiocarbon age of deposit-feeding molluscs in calcareous environments. Boreas 42, 362–373.

Evans, J., Pudsey, C.J., 2002. Sedimentation associated with Antarctic Peninsula ice shelves: implications for palaeoenvironmental reconstructions of glacimarine sediments. Journal of the Geological Society of London 159, 233–237.

Eyles, N., Eyles, C.H., Maill, A.D., 1983. Lithofacies types and vertical profile models; an alternative approach to the description and environmental interpretation of glacial diamict and diamictite sequences. Sedimentology 30, 393–410.

Fisher, D.A., Koerner, R.M., 2003. Holocene ice-core climate history — a multi-variable approach. In: Battarbee, R. (Ed.), Global Change in the Holocene. Hodder Arnold, London, pp. 281–293.

Fisher, D.A., Koerner, R.M., Reeh, N., 1995. Holocene climatic records from Agassiz Ice Cap, Ellesmere Island, NWT, Canada. The Holocene 5, 19–24.

Forman, S.L., Polyak, L., 1997. Radiocarbon content of pre-bomb marine mollusks and variations in the ^{14}C reservoir age for coastal areas of the Barents and Kara seas, Russia. Geophysical Research Letters 24, 885–888.

Furze, M.F.A., Pieńkowski, A.J., England, J.H., 2010. Comment: Holocene palaeoceanographic changes in Barrow Strait, Canadian Arctic: foraminiferal evidence by Gregory et al., 2010. Journal of Quaternary Science 25, 1189–1192.

Furze, M.F.A., Pieńkowski, A.J., Coulthard, R.D., 2013. New cetacean ΔR values for Arctic North America and their implications for marine-mammal-based palaeoenvironmental reconstructions. Quaternary Science Reviews (submitted for publication).

Gajewski, K., 1995. Modern and Holocene pollen assemblages from some small Arctic lakes on Somerset Island, NWT, Canada. Quaternary Research 44, 228–236.

Gajewski, K., Atkinson, D.A., 2003. Climatic Change in northern Canada. Environmental Review 11, 69–102.

Gajewski, K., Vance, R., Sawada, M., Fung, I., Gignac, L.D., Halsey, L., John, J., Maisongrande, P., Mandell, P., Mudie, P.J., Richard, P.J.H., Sherin, R.A.G., Soroko, J., Vitt, D., 2000. The climate of North America and adjacent ocean waters ca. 6 ka. Canadian Journal of Earth Sciences 37, 661–681.

Gilbert, R., Nielsen, N., Möller, H., Desloges, J.R., Rasch, M., 2002. Glacimarine sedimentation in Kangerdluk (Disko Fjord), West Greenland, in response to a surging glacier. Marine Geology 191, 1–18.

Gordillo, S., Aitken, A.E., 2001. Postglacial succession and palaeoecology of Late Quaternary macrofaunal assemblages from the central Canadian Arctic Archipelago. Boreas 30, 61–72.

Green, K.E., 1960. Ecology of some Arctic Foraminifera. Micropaleontology 6, 57–78.

Gregory, T.R., Smart, C.W., Hart, M.B., Massé, G., Vare, L.L., Belt, S.T., 2010. Holocene palaeoceanographic changes in Barrow Strait, Canadian Arctic: foraminiferal evidence. Journal of Quaternary Science 25, 903–910.

Griffiths, S.D., Peltier, W.R., 2008. Megatides in the Arctic Ocean under glacial conditions. Geophysical Research Letters 35, L08605. http://dx.doi.org/10.1029/2008GL033263.

Hanslik, D., Jakobsson, M., Backman, J., Björck, S., Sellén, E., O'Regan, M., Fornaciari, E., Skog, G., 2010. Quaternary Arctic Ocean sea ice variations and radiocarbon reservoir age corrections. Quaternary Science Reviews 29, 3430–3441.

Head, M.J., Harland, R., Matthiessen, J., 2001. Cold marine indicators of the late Quaternary: the new dinoflagellate cyst genus *Islandinium* and related morphotypes. Journal of Quaternary Science 16, 621–636.

Hein, F.J., Mudie, P.J., 1991. Glacial-marine sedimentation, Canadian Polar Margin, north of Axel Heiberg Island. Géographie Physique et Quaternaire 45, 213–227.

Hein, F.J., van Wagner, N.A., Mudie, P.J., 1990. Sedimentary facies and processes of deposition: Ice Island cores, Axel Heiberg shelf, Canadian polar continental margin. Marine Geology 93, 243–265.

Hodgson, D.A., Vincent, J.S., 1984. A 10,000 yr. extensive ice shelf over Viscount Melville Sound, Arctic Canada. Quaternary Research 22, 18–30.

Holland, P.R., Feltham, D.L., Jenkins, A., 2007. Ice shelf water plume flow beneath Filchner–Ronne Ice Shelf, Antarctica. Journal of Geophysical Research, Oceans 112, C05044. http://dx.doi.org/10.1029/2006JC003915.

Howell, S.E.L., Duguay, C.R., Markus, T., 2009. Sea ice conditions and melt season duration variability within the Canadian Arctic Archipelago: 1979–2008. Geophysical Research Letters 36, L10502.

Hunt, A.S., Corliss, B.H., 1993. Distribution and microhabitats of living (stained) benthic Foraminifera from the Canadian Arctic Archipelago. Marine Micropaleontology 20, 321–345.

Hurlbut, S., 1997. Cruise Report, Cruise #9722, JOIS Transit Leg 3. Unpublished Geological Survey of Canada – Atlantic Report, 46pp.

Ingram, R.G., Prinsenberg, S., 1998. Coastal oceanography of Hudson Bay and surrounding eastern Canadian Arctic waters. In: Robinson, A.R., Brink, K.H. (Eds.), The Sea, Vol. 11: the Global Coastal Ocean, Regional Studies and Syntheses. Wiley, New York, pp. 835–862.

IPCC, 2007. Climate change 2007: the physical science basis. In: Solomon, S., Qin, D., Manning, M., Chen, Z., Marquis, M., Averyt, K.B., Tignor, M., Miller, H.L. (Eds.), Contribution of Working Group I to the Fourth Assessment Report of the Intergovernmental Panel on Climate Change. Cambridge University Press, Cambridge, p. 996.

Jaeger, J.M., Nittrouer, C.A., 1999. Marien record of surge-induced outburst floods from the Bering Glacier, Alaska. Geology 27, 847–850.

Jakobsson, M., Macnab, R., Mayer, L., Anderson, R., Edwards, M., Hatzky, J., Schenke, H.W., Johnson, P., 2008. An improved bathymetric portrayal of the Arctic Ocean: implications for ocean modelling and geological, geophysical and oceanographic analyses. Geophysical Research Letters 35, L07602. http://dx.doi.org/10.1029/2008GL033520.

Jennings, A., Weiner, N.J., Helgadottir, G., Andrews, J.T., 2004. Modern foraminiferal faunas of the southwestern to northern Iceland shelf: oceanographic and environmental controls. Journal of Foraminiferal Research 34, 180–207.

Jennings, A.E., Hald, M., Smith, M., Andrews, J.T., 2006. Freshwater forcing from the Greenland Ice Sheet during the Younger Dryas: evidence from southeastern Greenland shelf cores. Quaternary Science Reviews 25, 282–298.

Jennings, A., Andrews, J., Wilson, L., 2011. Holocene environmental evolution of the SE Greenland Shelf North and South of the Denmark Strait: Irminger and East Greenland current interactions. Quaternary Science Reviews 30, 980–998.

Jones, E.P., 2001. Circulation in the Arctic Ocean. Polar Research 20, 139–146.

Jones, E.P., Coote, A.R., 1980. Nutrient distributions in the Canadian Archipelago: indicators of summer water mass and flow characteristics. Canadian Journal of Fisheries and Aquatic Sciences 37, 589–599.

Jones, E.P., Swift, J.H., Anderson, L.G., Lipizer, M., Civitarese, G., Falkner, K.K., Kattner, G., McLaughlin, F., 2003. Tracing Pacific water in the North Atlantic Ocean. Journal of Geophysical Research 108. http://dx.doi.org/10.1029/2001JC001141.

Kaufman, D.S., Ager, T.A., Anderson, N.J., Anderson, P.M., Andrews, J.T., Bartlein, P.J., Brubaker, L.B., Coats, L.L., Cwynar, L.C., Duvall, M.L., Dyke, A.S., Edwards, M.E., Eisner, W.R., Gajewski, K., Geirsdóttir, A., Hu, F.S., Jennings, A.E., Kaplan, M.R., Kerwin, M.W., Lozhkin, A.V., MacDonald, G.M., Miller, G.H., Mock, C.J., Oswald, W.W., Otto-Bliesner, B.L., Porinchu, D.F., Rühland, K., Smol, J.P., Steig, E.J., Wolfe, B.B., 2004. Holocene thermal maximum in the western Arctic (0–180°W). Quaternary Science Reviews 23, 529–560.

Kellogg, T.B., Kellogg, D.E., 1998. Antarctic cryogenic sediments: biotic and inorganic facies of ice shelf and marine-based ice sheet environments. Palaeogeography, Palaeoclimatology, Palaeoecology 67, 51–74.

Knudsen, K.L., Stabell, B., Seidenkrantz, M.-S., Eiríkson, J., Blake Jr., W., 2008. Deglacial and Holocene conditions in northernmost Baffin Bay: sediments, foraminifera, diatoms and stable isotopes. Boreas 37, 346–376.

Koerner, R.M., Fisher, D.A., 1990. A record of Holocene summer climate from a Canadian high-Arctic ice core. Nature 343, 630–631.

Koerner, R.M., Fisher, D.A., 2002. Ice core evidence for widespread Arctic glacier retreat in the Last Interglacial and the early Holocene. Annals of Glaciology 35, 19–24.

Korsun, S., Hald, M., 1998. Modern benthic Foraminifera off tide water glaciers, Novaja Semlja, Russian Arctic. Arctic and Alpine Research 30, 61–77.

Kunz-Pirrung, M., 1998. Rekonstruktion der Oberflächenmassen der östlichen Laptevsee im Holozän anhand aquatischen Palynomorphen. Berichte zür Polarforschung 281, 1–116.

Leblond, P.H., 1980. On the surface circulation in some channels of the Canadian Arctic Archipelago. Arctic 33, 189–197.

Ledu, L., Rochon, A., de Vernal, A., St-Onge, G., 2008. Palynological evidence of Holocene climate change in the eastern Arctic: a possible shift in the Arctic oscillation at the millennial time scale. Canadian Journal of Earth Sciences 45, 1363–1375.

Ledu, D., Rochon, A., de Vernal, A., Barletta, F., St-Onge, G., 2010a. Holocene sea ice history and climate variability along the main axis of the Northwest Passage, Canadian Arctic. Paleoceanography 25, PA2213. http://dx.doi.org/10.1029/2009PA001817.

Ledu, D., Rochon, A., de Vernal, A., St-Onge, G., 2010b. Holocene paleoceanography of the northwest passage, Canadian ArcticArchipelago. Quaternary Science Reviews 29, 3468–3488.

Levinsen, H., Nielsen, T.G., 2002. The trophic role of marine pelagic ciliates and heterotrophic dinoflagellates in Arctic and temperate coastal ecosystems: a cross-latitude comparison. Limnology and Oceanography 47, 427–439.

Licht, K.J., Jennings, A.E., Andrews, J.T., Williams, K.M., 1996. Chronology of late Wisconsin ice retreat from the western Ross Sea, Antarctica. Geology 24, 223–226.

Licht, K.J., Dunbar, N.W., Andrews, J.T., Jennings, A.E., 1999. Distinguishing subglacial till and glacial marine diamictons in the western Ross Sea, Antarctica: implications for a last glacial maximum grounding line. GSA Bulletin 111, 91–103.

Lloyd, J.M., Kuijpers, A., Long, A., Moros, M., Park, L.A., 2007. Foraminiferal reconstruction of mid- to late-Holocene ocean circulation and climate variability in Disko Bugt, West Greenland. The Holocene 17, 1079–1091.

Mackensen, A., Sejrup, H., Jansen, E., 1985. The distribution of living and dead benthic foraminifera on the continental slope and rise off southwest Norway. Marine Micropaleontology 9, 275–306.

MacLean, B., Vilks, G., 1986. Marine geological program in the Byam Martin Channel — Lougheed Island region, District of Franklin. Geological Survey of Canada Paper 86-1A, 769–777.

MacLean, B., Sonnichsen, G., Vilks, G., Powell, C., Moran, K., Jennings, A., Hodgson, D., Deonarine, B., 1989. Marine geological and geotechnical investigations in Wellington, Byam Martin, Austin, and adjacent channels, Canadian Arctic Archipelago. Geological Survey of Canada Paper 89–11, 1–69.

MacLean, B., Blasco, S., Bennett, R., England, J., Rainey, W., Hughes-Clarke, J., Beaudoin, J., 2010. Ice keel seabed sculpturing in marine channels of the central Canadian Arctic Archipelago: evidence for former ice streams and iceberg scouring. Quaternary Science Reviews 29, 2280–2301.

Marret, F., Zonneveld, K., 2003. Atlas of modern organic-walled dinoflagellate cyst distribution. Review of Palaeobotany and Palynology 125, 1–200.

Matthiessen, J., de Vernal, A., Head, M., Okolodkov, Y., Zonneveld, K., Harland, R., 2005. Modern organic-walled dinoflagellate cysts and their (paleo-)environmental significance. Paläontologische Zeitschrift 79, 3–51.

Melling, H., 2000. Exchanges of freshwater through the shallow straits of the North American Arctic. In: Lewis, E.L., Jones, E.P., Lemke, P., Prowse, T.D., Wadhams, P. (Eds.), The Freshwater Budget of the Arctic Ocean. Kluwer Academic Publishers, Dordrecht, pp. 479–502.

Melling, H., 2002. Sea ice of the northern Canadian Arctic Archipelago. Journal of Geophysical Research 107, 3181. http://dx.doi.org/10.1029/2001JC001102.

Melling, H., Francois, R., Myers, P.G., Perrie, W., Rochon, A., Taylor, R.L., 2012. The Arctic Ocean — a Canadian perspective from IPY. Climate Change. http://dx.doi.org/10.1007/s10584-012-0576-4.

Michel, C., Ingram, R.G., Harris, L.R., 2006. Variability in oceanographic and ecological processes in the Canadian Arctic Archipelago. Progress in Oceanography 71, 379–401.

Mortlock, R.A., Froelich, P.N., 1989. A simple method for the rapid determination of biogenic opal in pelagic marine sediments. Deep-Sea Research 36, 1415–1426.

Mudie, P.J., Harland, R., 1996. Aquatic Quaternary. In: Jansonius, J., McGregor, D.C. (Eds.), Palynology: Principles and Applications. American Association of Stratigraphic Palynologists Foundation, Dallas, pp. 843–877.

Mudie, P.J., Rochon, A., 2001. Distribution of dinoflagellate cysts in the Canadian Arctic marine region. Journal of Quaternary Science 16, 595–602.

Mudie, P.J., Short, S.K., 1985. Marine palynology of Baffin Bay. In: Andrews, J.T. (Ed.), Quaternary Environments: Eastern Canadian Arctic, Baffin Bay and West Greenland. George Allen and Unwin Ltd., London, pp. 263–308.

Mudie, P.J., Rochon, A., Levac, E., 2005. Decadal-scale sea ice changes in the Canadian Arctic and their impacts on humans during the past 4,000 years. Environmental Archaeology 10, 113–126.

Mudie, P.J., Rochon, A., Prins, M.A., Soenarjo, D., Troelstra, S.R., Levac, E., Scott, D.B., Roncaglia, L., Kuijpers, A., 2006. Late Pleistocene–Holocene marine geology of Nares Strait region: palaeoceanography from foraminifera and dinoflagellate cysts, sedimentology and stable isotopes. Polarforschung 74, 169–183.

Munk, W., 2003. Ocean freshening, sea level rising. Science 300, 2041–2043.

Ó Cofaigh, C., Dowdeswell, J.A., 2001. Laminated sediments in glacimarine environments: diagnostic criteria for their interpretation. Quaternary Science Reviews 20, 1411–1436.

Ockelmann, W.K., 1958. The zoology of East Greenland. Marine lamellibranchiata. Meddelelser om Grønland 122, 1–256.

Paterson, W.S.B., Koerner, R.M., Fisher, D., Johnsen, S.J., Clausen, H.B., Dansgaard, W., Bucher, P., Oeschger, H., 1977. An oxygen-isotope climatic record from the Devon Island ice cap, arctic Canada. Nature 266, 508–511.

Peros, M.C., Gajewski, K., 2009. Pollen-based reconstructions of late Holocene climate from the central and western Canadian Arctic. Journal of Paleolimnology 41, 161–175.

Pharand, D., 1984. The Northwest Passage Arctic straits. International Straits of the World, vol. 7. Martinus Nijhoff Publishers, Dordrecht.

Pieńkowski, A.J., Mudie, P.J., England, J.H., Smith, J.N., Furze, M.F.A., 2011. Late Holocene environmental conditions in Coronation Gulf, SW Canadian Arctic Archipelago: evidence from dinoflagellate cysts, other non-pollen palynomorphs, and pollen. Journal of Quaternary Science 26, 839–853.

Pieńkowski, A.J., England, J.H., Furze, M.F.A., Marret, F., Eynaud, F., Vilks, G., MacLean, B., Blasco, S., Scourse, J.D., 2012. The deglacial to postglacial marine environments of southeastern Barrow Strait, Canadian Arctic Archipelago. Boreas 41, 141–179.

Pieńkowski, A.J., England, J.H., Furze, M.F.A., MacLean, B., Blasco, S., 2013. The late Quaternary environmental evolution of marine Arctic Canada: Barrow Strait to Lancaster Sound. Quaternary Science Reviews (submitted for publication).

Polyak, L., Alley, R.B., Andrews, J.T., Brigham-Grette, J., Cronin, T.M., Darby, D.A., Dyke, A.S., Fitzpatrick, J.J., Funder, S., Holland, M., Jennings, A.E., Miller, G.H., O'Regan, M., Savelle, J., Serreze, M., St. John, K., White, J.W.C., Wolff, E., 2010. History of sea ice in the Arctic. Quaternary Science Reviews 29, 1757–1778.

Pospelova, V., Chmura, G.L., Walker, H.A., 2004. Environmental factors influencing the spatial distribution of dinoflagellate cyst assemblages in shallow lagoons of southern New England (USA). Review of Palaeobotany and Palynology 128, 7–34.

Pospelova, V., Chmura, G.L., Boothman, W.S., Latimer, J.S., 2005. Spatial distribution of modern dinoflagellate cysts in polluted estuarine sediments from Buzzards Bay (Massachusetts, USA) embayments. Marine Ecology Progress Series 292, 23–40.

Post, A.L., Hemer, M.A., O'Brien, P.E., Roberts, D., Craven, M., 2007. History of benthic colonisation beneath the Amery Ice Shelf, East Antarctica. Marine Ecology Progress Series 344, 29–37.

Prinsenberg, S.J., Bennett, E.B., 1987. Mixing and transports in Barrow Strait, the central part of the Northwest Passage. Continental Shelf Research 7, 913–935.

Reimer, P.J., Baillie, M.G.L., Bard, E., Bayliss, A., Beck, J.W., Blackwell, P.G., Bronk-Ramsey, C., Buck, C.E., Burr, G.S., Edwards, R.L., Friederich, M., Grootes, P.M., Guilderson, T.P., Hajdas, I., Heaton, T.J., Hogg, A.G., Hughen, K.A., Kaiser, K.F., Kromer, B., McCormac, F.G., Manning, S., Reimer, R.W., Richards, D.A., Southon, J.R., Talamo, S., Turney, C.S.M., van der Plicht, J., Weyhenmeyer, C.E., 2009. IntCal09 and Marine09 radiocarbon age calibration curves, 0–50,000 years cal BP. Radiocarbon 51, 1111–1150.

Richerol, T., Rochon, A., Blasco, S., Scott, D.B., Schell, T.M., Bennett, R.J., 2008. Evolution of paleo sea-surface conditions over the last 600 years in the Mackenzie Trough, Beaufort Sea (Canada). Marine Micropaleontology 68, 6–20.

Richerol, T., Pienitz, R., Rochon, A., 2012. Modern dinoflagellate cysts in surface sediments of Nunatsiavut fjords (Labrador, Canada). Marine Micropaleontology 88–89, 54–64.

Riedel, A., Michel, C., Poulin, M., Lessard, S., 2003. Taxonomy and abundance of microalgae and protists at a first-year sea ice station near Resolute Bay, Nunavut, Spring to early Summer 2001. Canadian Data Report of Hydrography and Ocean Sciences, 159, pp. 1–54.

Rochon, A., de Vernal, A., Turon, J.-L., Matthiessen, J., Head, M.J., 1999. Distribution of Recent dinoflagellate cysts in surface sediments from the North Atlantic Ocean and adjacent seas in relation to sea-surface parameters. American Association of Stratigraphic Palynologists: Foundation Contribution Series, 35 (152 pp.).

Roncaglia, L., 2004. New acritarch species from Holocene sediments in central West Greenland. Grana 43, 81–88.

Roncaglia, L., Kuijpers, A., 2004. Palynofacies analysis and organic-walled dinoflagellate cysts in late-Holocene sediments from Igaliku Fjord, South Greenland. The Holocene 14, 172–184.

Rudels, B., 1986. The outflow of polar water through the Arctic Archipelago and the oceanographic conditions in Baffin Bay. Polar Research 4, 161–180.

Schäfer, C.T., Cole, F.E., 1986. Reconnaisance survey of benthonic foraminifera from Baffin Island fiord environments. Arctic 39, 232–239.

Schell, T.M., Scott, D.B., Rochon, A., Blasco, S., 2008a. Late Quaternary paleoceanography and paleo-sea ice conditions in the Mackenzie Trough and Canyon, Beaufort Sea. Canadian Journal of Earth Sciences 45, 1399–1415.

Schell, T.M., Moss, T.J., Scott, D.B., Rochon, A., 2008b. Paleo-sea ice conditions of the Amundsen Gulf, Canadian Arctic Archipelago: Implications from the foraminiferal record of the last 200 years. Journal of Geophysical Research 113, C03S02. http://dx.doi.org/10.1029/2007JC004202.

Schröder-Adams, C.J., Cole, F.E., Medioli, F.S., Mudie, P.J., Scott, D.B., Dobbin, L., 1990. Recent Arctic shelf foraminifera: seasonally ice covered vs. perennially ice covered areas. Journal of Foraminiferal Research 20, 8–36.

Schumacher, S., 2001. Mikrohabitatansprüche benthischer Foraminiferen in Sedimenten des Südatlantiks (Microhabitat preferences of benthic foraminifera in South Atlantic Ocean sediments). Berichte zur Polar- und Meeresforschung 403, 1–151.

Scott, D.B., Mudie, P.J., Vilks, G., Younger, C.D., 1984. Latest Pleistocene–Holocene paleoceanographic trends on the continental margin of eastern Canada: foraminiferal, dinoflagellate, and pollen evidence. Marine Micropaleontology 9, 181–218.

Scott, D.B., Schell, T., St-Onge, G., Rochon, A., Blasco, S., 2009. Foraminiferal assemblage changes over the last 15,000 years on the Mackenzie–Beaufort Sea Slope and Amundsen Gulf, Canada: implications for past sea ice conditions. Paleoceanography 24, PA2219. http://dx.doi.org/10.1029/2007PA001575.

Seidenkrantz, M.-S., 1995. *Cassidulina neoteretis* new species (Foraminifera): stratigraphic marker for deep sea and outer shelf areas. Journal of Micropalaeontology 14, 145–157.

Sherr, E.B., Sherr, B.F., 2007. Heterotrophic dinoflagellates: a significant component of microzooplankton biomass and major grazers of diatoms in the sea. Marine Ecology Progress Series 352, 187–197.

Short, S.K., Andrews, J.T., Williams, K.M., Weiner, N.J., Elias, S.A., 1994. Late Quaternary marine and terrestrial environments, Northwestern Baffin Island, Northwest Territories. Géographie Physique et Quaternaire 48, 85–95.

Smith, L.M., Andrews, J.T., 2000. Sediment characteristics in iceberg dominated fjords, Kangerlussuaq region, East Greenland. Sedimentary Geology 130, 11–25.

Smol, J.P., Wolfe, A.P., Birks, H.J.B., Douglas, M.S.V., Jones, V.J., Korhola, A., Pienitz, R., Rühland, K., Sorvari, S., Antoniades, D., Brooks, S.J., Fallu, M.A., Hughes, M., Keatley, B.E., Laing, T.E., Michelutti, N., Nazarova, L., Nyman, M., Paterson, A.M., Perren, B., Quinlan, R., Rautio, M., Saulnier-Talbot, E., Siitoneni, S., Solovieva, N., Weckstrom, J., 2005. Climate-driven regime shifts in the biological communities of arctic lakes. Proceedings of the National Academy of Sciences of the United States of America 102, 4397–4402.

Stancliffe, R.P.W., 1991. Microforaminiferal linings. In: Jansonius, J., McGregor, D.C. (Eds.), Palynology: Principles and Applications. American Association of Stratigraphic Palynologists Foundation, Dallas, pp. 373–379.

Stockmarr, M., 1971. Tablets with spores used in absolute pollen analysis. Pollen et Spores 13, 615–621.

Stuiver, M., Polach, H.A., 1977. Reporting of ^{14}C data. Radiocarbon 19, 355–363.

Stuiver, M., Reimer, P.J., Reimer, R.W., 2013. CALIB 6.0 (WWW programme and documentation).

Tang, C.C.L., Ross, C.K., Yao, T., Petrie, B., DeTracey, B.M., Dunlap, E., 2004. The circulation, water masses and sea-ice of Baffin Bay. Progress in Oceanography 63, 183–228.

Thomsen, E., Vorren, T.O., 1986. Macrofaunal palaeoecology and stratigraphy in late Quaternary shelf sediments off northern Norway. Palaeogeography, Palaeoclimatology, Palaeoecology 56, 103–150.

Thorsteinsson, R., Kerr, J.W., 1967. Cornwallis Island and adjacent smaller islands, Canadian Arctic Archipelago. Geological Survey of Canada Paper 67–64, 1–16.

Trettin, H.P., 1989. The Arctic islands. In: Bally, A.W., Palmer, A.R. (Eds.), The Geology of North America: an Overview. Boulder, Colorado, Geological Society of America: The Geology of North America, vol. A, pp. 349–370.

Tricot, C., Berger, A., 1988. Sensitivity of present-day climate to astronomical forcing. In: Wanner, H., Siegenthaler, U. (Eds.), Long and Short Term Variability of Climate. Springer Verlag, Bern, pp. 132–152.

Vare, L.L., Massé, G., Gregory, T.R., Smart, C.W., Belt, S.T., 2009. Sea ice variations in the central Canadian Arctic Archipelago during the Holocene. Quaternary Science Reviews 28, 1354–1366.

Vilks, G., 1969. Recent Foraminifera in the Canadian Arctic. Micropaleontology 15 (1), 35–60.

Vilks, G., 1974. The distribution of planktonic Foraminifera in the sediments and water of the Northwest Passage and Northern Baffin Bay: a tool for paleoceanographic synthesis. Geological Survey of Canada Paper 74–30 (1), 109–121.

Vilks, G., 1989. Ecology of recent Foraminifera on the Canadian Continental Shelf of the Arctic Ocean. In: Herman, Y. (Ed.), The Arctic Seas: Climatology, Oceanography, Geology, and Biology. Van Nostrand Reinhold, New York, pp. 497–569.

von Prause, M.D., 2011. Foraminiferal linings: a new (palaeo)environmental tool in the Canadian Arctic Archipelago. Unpublished MSc thesis, Bangor University, 165pp.

Washburn, A.L., Stuiver, M., 1985. Radiocarbon dates from Cornwallis Island area, Arctic Canada — an interim report. Canadian Journal of Earth Sciences 22, 630–637.

White, J.W.C., Alley, R.B., Brigham-Grette, J., Fitzpatrick, J.J., Jennings, A.E., Johnsen, S.J., Miller, G.H., Nerem, R.S., Polyak, L., 2010. Past rates of climate change in the Arctic. Quaternary Science Reviews 29, 1716–1727.

Wollenburg, J.E., Mackensen, A., 1998. Living benthic foraminifers from the central Arctic Ocean: faunal composition, standing stock and diversity. Marine Micropaleontology 34, 153–185.

Zonneveld, K.A.F., Bockelmann, F.D., Holzwarth, U., 2007. Selective preservation of organic-walled dinoflagellate cysts as a tool to quantify past net primary production and bottom water oxygen concentrations. Marine Geology 237, 109–126.